TRANSACTIONS OF THE
AMERICAN MATHEMATICAL SOCIETY
Volume 369, Number 10, October 2017, Pages 7213–7250
http://dx.doi.org/10.1090/tran/6907
Article electronically published on June 27, 2017

IMMERSED SELF-SHRINKERS

GREGORY DRUGAN AND STEPHEN J. KLEENE

Abstract. We construct infinitely many complete, immersed self-shrinkers with rotational symmetry for each of the following topological types: the sphere, the plane, the cylinder, and the torus.

1. Introduction

In this paper, we construct infinitely many complete, immersed self-shrinkers with rotational symmetry in $\mathbb{R}^{n+1}$, $n \geq 2$.

Theorem 1. *There are infinitely many complete, immersed self-shrinkers in $\mathbb{R}^{n+1}$, $n \geq 2$, for each of the following topological types: the sphere (S^n), the plane ($\mathbb{R}^n$), the cylinder ($\mathbb{R} \times S^{n-1}$), and the torus ($S^1 \times S^{n-1}$).*

An immersion F from an n-dimensional manifold M into $\mathbb{R}^{n+1}$ is called a self-shrinker if it is a solution to

$$\Delta_g F = -\frac{1}{2} F^{\perp}, \tag{1}$$

where g is the metric on M induced by the immersion, Δ_g is the Laplace-Beltrami operator, and $F^{\perp}(p)$ is the projection of $F(p)$ into the normal space $N_p M$. The mean curvature of $F(M)$ is given by $\Delta_g F$, and when F is a self-shrinker, the family of submanifolds

$$M_t = \sqrt{-t} F(M)$$

is a solution to the mean curvature flow for $t \in (-\infty, 0)$. It is a consequence of Huisken's monotonicity formula [20] that a solution to the mean curvature flow behaves asymptotically like a self-shrinker at a type I singularity. In addition, self-shrinkers are minimal surfaces for the conformal metric $e^{-|x|^2/(2n)}(dx_1^2 + \ldots + dx_{n+1}^2)$ on $\mathbb{R}^{n+1}$.

Examples of self-shrinkers in $\mathbb{R}^{n+1}$, $n \geq 2$, include the sphere of radius $\sqrt{2n}$ centered at the origin, the plane through the origin, the cylinder with an axis through the origin and radius $\sqrt{2(n-1)}$, and an embedded torus ($S^1 \times S^{n-1}$) constructed by Angenent [3]. Numerical evidence for the existence of an immersed sphere self-shrinker was provided by Angenent [3] in 1989. In 1994, Chopp [6] described an algorithm for constructing surfaces that are approximately self-shrinkers and provided numerical evidence for the existence of a number of self-shrinkers, including compact, embedded self-shrinkers of genus 5 and 7. Recently, Kapouleas, the second

Received by the editors June 22, 2013 and, in revised form, November 12, 2015, December 28, 2015, and January 4, 2016.

2010 *Mathematics Subject Classification.* Primary 53C44, 53C42.

Key words and phrases. Mean curvature flow, self-shrinker.

The first author was partially supported by NSF RTG 0838212.

The second author was partially supported by NSF DMS 1004646.

author, and Møller [21] and Nguyen [24]–[26] used desingularization constructions to produce examples of complete, non-compact, embedded self-shrinkers with high genus in $\mathbb{R}^3$. Møller [23] also used desingularization techniques to construct compact, embedded, high genus self-shrinkers in $\mathbb{R}^3$. In [10], the first author constructed an immersed sphere self-shrinker.

In contrast to these constructions are several rigidity theorems for self-shrinkers. Huisken [20] showed that the sphere of radius $\sqrt{2n}$ is the only compact, mean-convex self-shrinker in $\mathbb{R}^{n+1}$, $n \geq 2$. In their study of generic singularities of the mean curvature flow, Colding and Minicozzi [7] showed that the only F-stable[1] self-shrinkers with polynomial volume growth in $\mathbb{R}^{n+1}$, $n \geq 2$, are the sphere of radius $\sqrt{2n}$ and the plane. Ecker and Huisken [12] showed that an entire self-shrinker graph with polynomial volume growth must be a plane in their study of the mean curvature flow of entire graphs. Afterwards, Lu Wang [27] showed that an entire self-shrinker graph has polynomial volume growth. In [9], the first author showed that an embedded sphere self-shrinker with rotational symmetry is mean-convex, so by Huisken's result, it must be the sphere of radius $\sqrt{2n}$. In their classification of complete, embedded self-shrinkers with rotational symmetry, the second author and Møller [22] showed that the sphere of radius $\sqrt{2n}$, the plane, and the cylinder of radius $\sqrt{2(n-1)}$ are the only embedded, rotationally symmetric self-shrinkers of their respective topological type.

The self-shrinkers we study in this paper are hypersurfaces with rotational symmetry about a line through the origin in $\mathbb{R}^{n+1}$. Such a hypersurface may be expressed as $F(s,\omega) = (x(s), r(s)\omega)$, where $(x(s), r(s))$ is a curve in the upper half-plane $\{(x,r) : x \in \mathbb{R}, r > 0\}$ and $\omega \in S^{n-1}$. In this setting, the self-shrinker equation (1) reduces to the second order differential equation

$$\frac{x'r'' - r'x''}{x'^2 + r'^2} - \frac{n-1}{r}x' = -\frac{1}{2}\left(rx' - xr'\right), \tag{2}$$

and the proof of Theorem 1 reduces to the construction of solutions to (2) that correspond to complete self-shrinkers with rotational symmetry (see Figure 1 and Appendix C). In addition, solutions to (2) are geodesics for the conformal metric

$$g_{Ang} = r^{2(n-1)}e^{-(x^2+r^2)/2}(dx^2 + dr^2)$$

on the upper half-plane.

The heuristic for the constructions of self-shrinkers in this paper is to study the behavior of solutions to (2) near the profile curves for two known complete self-shrinkers and use continuity arguments to find complete self-shrinkers between them. To implement this heuristic, we organize the paper as follows.

In Section 2, we introduce the differential equations that we study in the paper. Most of the analysis in this paper deals with solutions to (2) written as graphs over the x-axis or the r-axis. Here, we discuss some immediate consequences of these equations, including the basic shape of solutions written as graphs over the x-axis. We also show that a non-linear solution to (2) is strictly convex in the Euclidean sense at any point where it has a vertical or horizontal tangent. In addition, we prove some crossing and blow-up results for solutions on intervals where they are

[1]Self-shrinkers are unstable as minimal surfaces on $\mathbb{R}^{n+1}$ for the conformal metric $e^{-|x|^2/(2n)}(dx_1^2 + \ldots + dx_{n+1}^2)$, which can be seen by translating a self-shrinker in space (or time). To account for these translations when considering the stability of self-shrinkers, Colding and Minicozzi introduced the notion of F-stability (see [7], p. 763).

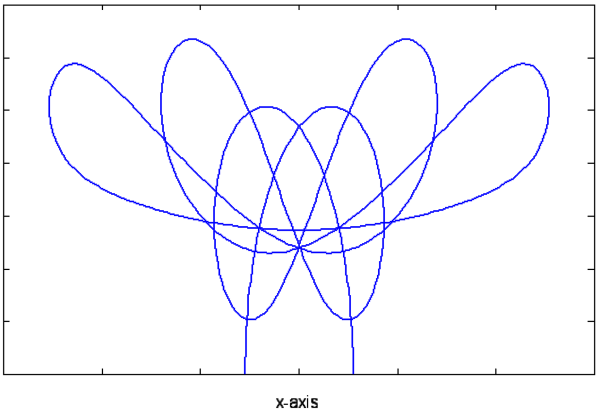

FIGURE 1. A profile curve whose rotation about the x-axis is an immersed sphere self-shrinker.

convex. We end the section by stating the Gauss-Bonnet formula for the conformal metric g_{Ang} on the upper half-plane. A new feature in this paper is the use of the Gauss-Bonnet formula to control the behavior of solutions that almost exit the upper half-plane.

In Section 3, we focus on the structure of solutions to (2) written as graphs over the x-axis. We begin by describing a decomposition of a solution into its graphical components. We refer to the image of such a graphical component as a *graphical geodesic segment*, and the main goal of this section is to establish a structure result for these graphical geodesic segments. This is essentially proved in Proposition 3, which shows that the Euclidean curvature of a non-linear solution to (2), written as a graph over the x-axis, can vanish at no more than two points. In this section, we also introduce the set of *half-entire graphs*, whose elements are the maximally extended graphical geodesic segments that are not compactly contained in the upper half-plane. These half-entire graphs provide a key component in our construction of complete self-shrinkers. In fact, the continuity arguments developed in this paper are focused on finding solutions to (2) whose decompositions into graphical geodesic segments begin and end with half-entire graphs. We finish the section with Proposition 6, which classifies the half-entire graphs into their different types.

In Section 4 we introduce the two shooting problems for (2) that we study in this paper. In one of the shooting problems, we shoot perpendicularly from the x-axis, and in the other, we shoot perpendicularly from the r-axis. In both cases, the goal is to find a solution to (2) that eventually has a graphical geodesic segment that is a half-entire graph. Such a solution will be the profile curve for a complete self-shrinker with rotational symmetry. In addition, a solution to either of these shooting problems that eventually intersects the r-axis perpendicularly will also be the profile curve for a complete self-shrinker.

In Section 5, we study the limiting properties of solutions to (2). Our first observation is that whenever a continuous family of graphical geodesic segments changes type, it must do so through a half-entire graph. This observation will be used in conjunction with the shooting method to find new examples of complete self-shrinkers between two known examples. The main result in this section is

Proposition 7, which shows that whenever a continuous family of graphical geodesic segments converges to a half-entire graph, the corresponding solutions to (2) converge to this half-entire graph with multiplicity. Roughly speaking, this result says that when a family of solutions converges to a half-entire graph, they will follow the half-entire graph as it exits the upper half-plane, turn around, and return back along the same half-entire graph. The proof of Proposition 7 involves the application of the Gauss-Bonnet formula to the metric g_{Ang}. Several convergence results are collected in Corollary 1.

In Section 6, we continue our study of the two shooting problems. In Proposition 8 and Proposition 9 we describe the asymptotic behavior of solutions near the profile curves of the plane and the cylinder, respectively. The proofs of these results rely heavily on the analysis and techniques developed in the previous sections. Then we illustrate our method by implementing two procedures for constructing self-shrinkers. We prove the result from [3] that there is an embedded torus self-shrinker and the result from [10] that there is an immersed sphere self-shrinker. We finish this section by describing the asymptotic behavior of solutions near Angenent's torus.

In Section 7, we complete our construction of self-shrinkers with rotational symmetry. We construct an infinite number of sphere and plane self-shrinkers near the plane, an infinite number of sphere and torus self-shrinkers near the cylinder, and an infinite number of sphere and cylinder self-shrinkers near Angenent's torus. The proofs of the results in this section use induction arguments that utilize the asymptotic behaviors described in Section 6 and the convergence properties established in Section 5.

We note that in the one-dimensional case, the self-shrinking solutions to the curve shortening flow have been completely classified (see Gage and Hamilton [14], Grayson [16], Abresch and Langer [1], Epstein and Weinstein [13], and Halldorsson [17]). One difficulty in higher dimensions ($n \geq 2$) is the presence of the $(n-1)/r$ term in (2), which allows the Euclidean curvature of a solution to change sign and forces a solution intersecting the axis of rotation $\{r = 0\}$ to do so perpendicularly.

We also note that the existence of immersed S^2 self-shrinkers shows that the uniqueness results for constant mean curvature spheres in $\mathbb{R}^3$ (see Hopf [19]) and for minimal spheres in S^3 (see Almgren [2]) do not hold for self-shrinkers. Very recently Brendle [5] has proved the longstanding conjecture that an embedded S^2 self-shrinker in $\mathbb{R}^3$ must be the sphere of radius 2. When $n \geq 3$, it is unknown whether or not the sphere of radius $\sqrt{2n}$ is the only embedded S^n self-shrinker in $\mathbb{R}^{n+1}$.

2. Preliminaries

In this section, we begin our study of self-shrinkers in $\mathbb{R}^{n+1}$, $n \geq 2$, with rotational symmetry about a line through the origin. We can describe such a self-shrinker as $F(s, \omega) = (x(s), r(s)\omega)$, where $(x(s), r(s))$ is a curve in the upper half-plane $\mathbb{H} = \{(x, r) : x \in \mathbb{R},\, r > 0\}$ and $\omega \in S^{n-1}$. In this case, the self-shrinker equation (1) is equivalent to the second order differential equation

$$\frac{x'r'' - r'x''}{x'^2 + r'^2} = \frac{x}{2}r' + \left(\frac{n-1}{r} - \frac{r}{2}\right)x'. \tag{3}$$

We will refer to the curve $(x(s), r(s))$ as the *profile curve* for the self-shrinker $F(s, \omega)$. We note that a self-shrinker with rotational symmetry may intersect its axis of rotation, in which case the profile curve will intersect the x-axis orthogonally. We also note that the reflection of a solution to (3) about the r-axis is a solution to (3). In particular, if a solution to (3) intersects the r-axis orthogonally, then it is symmetric with respect to reflections about the r-axis.

The simplest examples of solutions to (3) are the line $(0, s)$, the line $(s, \sqrt{2(n-1)})$ and the the semicircle $\sqrt{2n}(\cos(s), \sin(s))$. As they are profile curves for an $\mathbb{R}^n$ self-shrinker, an $\mathbb{R} \times S^{n-1}$ self-shrinker, and an S^n self-shrinker, we will refer to the images of these special profile curves as $\mathcal{P}$, $\mathcal{C}$, and $\mathcal{S}$, respectively.

Using the shooting method for differential equations, Angenent [3] discovered a solution to (3) whose image is a simple, closed convex curve. This solution corresponds to an embedded $S^1 \times S^{n-1}$ self-shrinker. It is unknown if this example is the only embedded $S^1 \times S^{n-1}$ self-shrinker; however, it is known (up to an orthogonal transformation of $\mathbb{R}^{n+1}$) that the flat plane through the origin, the round cylinder of radius $\sqrt{2(n-1)}$ with axis through the origin, and the round sphere of radius $\sqrt{2n}$ centered at the origin are the only complete, embedded, rotationally symmetric self-shrinkers of their respective topological type (see [9] and [22]).

Other examples of solutions to (3) include a one parameter family of solutions, called trumpets, constructed by the second author and Møller in [22, Theorem 3]. Each solution has a convex end that is asymptotic from above to a unique ray through the origin in $\mathbb{H}$. The rotation of this end about the x-axis has the appearance of an infinite trumpet. In [10], the first author constructed an immersed (and non-embedded) sphere self-shrinker using the shooting method for solutions to (3) that intersect the x-axis orthogonally.

2.1. **Equations.** Let $\gamma : I \to \mathbb{H}$ be a solution to (3), and let $\Gamma = \gamma(I)$ denote the image of this curve. We note that the shooting problems we study do take into account the given parametrization of the solution γ. However, much of the analysis in this paper is focused on the image of the curve. In this section, we introduce the equations we use to describe the possible shapes of Γ.

2.1.1. *Graphs over the x-axis.* Writing Γ locally as the graph of a function $u(x)$ over the x-axis, it follows from (3) that $u(x)$ satisfies the non-linear differential equation

$$\frac{u''}{1+u'^2} = \frac{xu'}{2} + \frac{n-1}{u} - \frac{u}{2}. \tag{4}$$

Differentiating (4), we have

$$\frac{u'''}{1+(u')^2} = \frac{2u'(u'')^2}{(1+(u')^2)^2} + \frac{xu''}{2} - \frac{n-1}{u^2}u'. \tag{5}$$

When $u(x)$ is a solution to (4), we have the following implications:

$$u'(x_0) = 0 \qquad \Longrightarrow \qquad u''(x_0) = \frac{n-1}{u(x_0)} - \frac{u(x_0)}{2}$$

and

$$u''(x_0) = 0 \qquad \Longrightarrow \qquad \frac{u'''(x_0)}{1+u'(x_0)^2} = -\frac{n-1}{u(x_0)^2}u'(x_0).$$

Notice that when $u'(x_0) = 0$, the value of $u(x_0)$ determines the local behavior of $u(x)$ near x_0. If $u'(x_0) = 0$ and $u(x_0) > \sqrt{2(n-1)}$ $(< \sqrt{2(n-1)})$, then u has a local minimum (maximum) at x_0. If $u'(x_0) = 0$ and $u(x_0) = \sqrt{2(n-1)}$, then $u(x) \equiv \sqrt{2(n-1)}$ is the constant solution corresponding to the cylinder self-shrinker. Also, notice that if both u' and u'' vanish at the same point, then $u \equiv \sqrt{2(n-1)}$.

Next, using the property that u' and u''' have opposite signs at points where $u'' = 0$, we see that the zeros of u'' are separated by zeros of u'. Here is a maximum principle proof of this observation.

Lemma 1. *Let u be a non-linear solution to (4) and suppose there exist $x_1 < x_2$ so that $u''(x_1) = u''(x_2) = 0$. Then there is a point $x_0 \in (x_1, x_2)$ so that $u'(x_0) = 0$.*

Proof. If $u' \neq 0$ in (x_1, x_2), then either u' or $-u'$ satisfies a maximum principle; see equation (5). Since u is non-linear and u' is non-constant, the strong maximum principle forces either u' or $-u'$ to achieve its maximum on the boundary of (x_1, x_2). But, this contradicts the Hopf boundary lemma since $u''(x_1) = u''(x_2) = 0$. Therefore, there is a point $x_0 \in (x_1, x_2)$ so that $u'(x_0) = 0$. □

Again using the property that u' and u''' have opposite signs at points where $u'' = 0$, we see that an increasing solution to (4) cannot change from concave down to concave up (and a decreasing solution cannot change from concave up to concave down). The basic shape and possible oscillatory behavior of a non-linear solution to (4) are completely determined by the previous observations. In Proposition 3 below, we show that the second derivative of a non-linear solution to (4) can vanish at no more than two points.

2.1.2. *Graphs over the r-axis.* In the setting where Γ is written locally as the graph of a function $f(r)$ over the r-axis, it follows from (3) that $f(x)$ satisfies

$$\frac{f''}{1+(f')^2} = \left(\frac{r}{2} - \frac{n-1}{r}\right) f' - \frac{f}{2} \tag{6}$$

and

$$\frac{f'''}{1+(f')^2} = \frac{2f'(f'')^2}{(1+(f')^2)^2} + \left(\frac{r}{2} - \frac{n-1}{r}\right) f'' + \frac{n-1}{r^2} f'. \tag{7}$$

If $f(r)$ is a solution to (6), then the following implications hold:

$$f'(r_0) = 0 \qquad \Longrightarrow \qquad f''(r_0) = -\frac{f(r_0)}{2}$$

and

$$f''(r_0) = 0 \qquad \Longrightarrow \qquad \frac{f'''(r_0)}{1+f'(r_0)^2} = \frac{n-1}{r_0^2} f'(r_0).$$

Notice that when $f'(r_0) = 0$, the sign of $f(r_0)$ determines the local behavior of $f(r)$ near r_0. Also, notice that an increasing solution cannot change from concave up to concave down (and a decreasing solution cannot change from concave down to concave up). We note that the (singular) shooting problem: $f(0) = f_0$, $f'(0) = 0$ was studied in [9] and [10].

Finally, we emphasize one feature of solutions to (3) that follows from the previous analysis. At any point where a non-linear solution to (3) has a vertical or horizontal tangent, the solution is strictly convex in the Euclidean sense.

2.2. **Behavior of convex solutions.** Here we focus on crossing and blow-up results for solutions to (4) and (6) on intervals where they are convex. We begin with the following lemma about solutions to (6), which shows that a positive, decreasing, concave down solution cannot be defined on an interval of the form $[\sqrt{2(n-1)}, M)$, for arbitrarily large M.

Lemma 2. *There exists $M_1 > \sqrt{2(n-1)}$ with the following property: Let f be a solution to (6) with $f(\sqrt{2(n-1)}) > 0$. Suppose $f'(r) \leq 0$ when $r \geq \sqrt{2(n-1)}$. Then $f(r) < 0$ whenever $r > M_1$ and $f(r)$ is defined.*

Proof. Notice that $f''(r) < 0$ when $r \geq \sqrt{2(n-1)}$, $f(r) > 0$, and $f'(r) \leq 0$. Also, $f'''(r) \leq 0$ when $r \geq \sqrt{2(n-1)}$, $f'(r) \leq 0$, and $f''(r) < 0$. The idea of the proof is to use this concave down behavior to force f to be negative when r is large enough. Choose $r > \sqrt{2(n-1)}$ so that $f > 0$ on $[\sqrt{2(n-1)}, r]$. Then

$$f''(r) \leq f''(\sqrt{2(n-1)}) \leq \frac{f''(\sqrt{2(n-1)})}{1 + f'(\sqrt{2(n-1)})^2} = -\frac{1}{2} f(\sqrt{2(n-1)}),$$

where we have used $f''' \leq 0$ on $[\sqrt{2(n-1)}, r]$, $f''(\sqrt{2(n-1)}) < 0$, and equation (4). Integrating twice from $\sqrt{2(n-1)}$ to r, we have

$$f(r) \leq f(\sqrt{2(n-1)}) \left[1 - \frac{1}{4}(r - \sqrt{2(n-1)})^2\right].$$

Choose $M_1 = 2 + \sqrt{2(n-1)}$. Then $f(r) < 0$ whenever $r > M_1$ and $f(r)$ is defined. □

Next, we prove a lemma about solutions to (6), which shows that a positive, increasing, concave down solution cannot be defined on an interval of the form $(m, \sqrt{2(n-1)}]$, for arbitrarily small m.

Lemma 3. *There exists $m_1 > 0$ with the following property: Let f be a solution to (6) with $f(\sqrt{2(n-1)}) > 0$. Suppose $f'(r) > 0$ and $f''(r) < 0$ when $r < \sqrt{2(n-1)}$. Then $f(r) < 0$ whenever $r < m_1$ and $f(r)$ is defined.*

Proof. The idea of the proof is to use the f'/r term to force f to be negative when r is small. We break the proof up into two steps.

Step 1. Estimate f' in terms of f at some point less than $\sqrt{2(n-1)}$. Without loss of generality, we assume that $f(1)$ is defined and positive. Using equation (7), we see that $f'''(r) > 0$ when $r < \sqrt{2(n-1)}$ (since $f'(r) > 0$ and $f''(r) < 0$). Then, for $r < \sqrt{2(n-1)}$, we see that $f''(r) \leq f''(\sqrt{2(n-1)})$. Using equation (6) and the positivity of f', we have $f''(\sqrt{2(n-1)}) \leq -\frac{1}{2} f(\sqrt{2(n-1)}) \leq -\frac{1}{2} f(1)$. Therefore, $f''(r) \leq -\frac{1}{2} f(1)$. Integrating from 1 to $\sqrt{2(n-1)}$, we arrive at the estimate

$$f'(1) \geq \frac{\sqrt{2(n-1)} - 1}{2} f(1).$$

Step 2. Estimate $f(r)$ for $r < 1$. Suppose $f > 0$ on $[r, 1]$. Then using $f' > 0$, $f'' < 0$, and (6), we have

$$\frac{f''(r)}{f'(r)} \leq -\frac{n-1}{r}.$$

Integrating from r to 1,

$$f'(r) \geq \frac{f'(1)}{r^{n-1}} \geq c_n \frac{f(1)}{r^{n-1}},$$

and integrating again

$$f(r) \leq f(1)\left[1 - c_n \int_r^1 \frac{1}{t^{n-1}} dt\right].$$

Choose m_1 so that $\int_{m_1}^1 \frac{1}{t^{n-1}} dt \geq 1/c_n$. Then $f(r) < 0$ whenever $r < m_1$ and $f(r)$ is defined.

□

We also prove the following blow-up result for convex solutions to (4).

Lemma 4. *Let $u : [x_0, b) \to (0, \infty)$ be a solution to (4) with*

$$u(x_0) < \sqrt{2(n-1)}, \quad u'(x_0) = 0,$$

where $x_0 \geq 0$ and $b < \infty$. If $u''(x) > 0$ for $x \in [x_0, b)$, then $\lim_{x\to b} u(x) < \infty$.

Proof. Suppose to the contrary that $\lim_{x\to b} u(x) = \infty$. Then there is a point $x_1 > x_0$ for which $u(x_1) = x_1 u'(x_1)$. (If no such point exists, then $0 < u'(x) < u(x)/x$ for $x_0 < x < b$. Integrating from say $(b + x_0)/2$ to b shows that $u(b)$ is bounded, which is a contradiction.)

We consider the function $\Psi(x) = xu' - u$ (from [22, Lemma 1]). If $x > x_0 \geq 0$, then $\Psi' = xu'' > \frac{1}{2}x(1 + (u')^2)\Psi$. Since $\Psi(x_1) = 0$, it follows that $\Psi(x) > 0$ and $\Psi'(x) > 0$ when $x > x_1$. In particular, we note that $u''/(1 + (u')^2) \geq (n-1)/u$ when $x > x_1$.

We will use a third derivative argument to show $\lim_{x\to b} u(x) < \infty$. Let $\psi = u'$. Then $\psi > 0$ and $\psi' > 0$ on (x_1, b), and $\psi(x_1) = \frac{u(x_1)}{x_1}$. Using equation (5), for $x > x_1$, we have

$$\psi'' \geq \frac{1}{2} x_1 \psi' \psi^2,$$

where we also used $u''/(1 + (u')^2) \geq (n-1)/u$ when $x > x_1$.

Now, for small $\varepsilon > 0$, consider the function

$$\phi_\varepsilon(x) = \frac{M}{\sqrt{b - \varepsilon - x}}.$$

We choose $M > 0$ so that $\frac{u(x_1)}{x_1} \leq \frac{M}{\sqrt{b-x_1}}$ and $\frac{3}{M^2} \leq x_1$. Then

$$\phi_\varepsilon'' \leq \frac{1}{2} x_1 \phi_\varepsilon' \phi_\varepsilon^2,$$

and $\phi_\varepsilon(x_1) > \psi(x_1)$. Suppose $\phi_\varepsilon - \psi$ is negative at some point in $(x_1, b - \varepsilon)$. Since $\phi_\varepsilon(x_1) > \psi(x_1)$ and $\phi_\varepsilon(b - \varepsilon) = \infty$, we know that $\phi_\varepsilon - \psi$ achieves a negative minimum at some point $x_0 \in (x_1, b - \varepsilon)$. Computing $(\phi_\varepsilon - \psi)''$ at x_0, we arrive at a contradiction:

$$0 \leq (\phi_\varepsilon - \psi)''(x_0) \leq \frac{1}{2} x_1 \phi_\varepsilon'(\phi_\varepsilon^2 - \psi^2)(x_0) < 0.$$

Therefore, $\psi \leq \phi_\varepsilon$. Taking $\varepsilon \to 0$ and integrating we see that u is bounded from above at b. □

2.3. **Gauss-Bonnet formula.** In [3, pp. 27-29], it was observed that a solution to (2) gives a parametrization of a geodesic for the conformal metric

$$g_{Ang} = r^{2(n-1)}e^{-(x^2+r^2)/2}(dx^2 + dr^2)$$

on the upper half-plane. In this way, we may regard Γ as the image of a geodesic for the metric g_{Ang}. We note that applying the Gauss-Bonnet formula (see [8, p. 274]) to a simple, compact region R in the upper half-plane whose boundary is the piecewise smooth union of geodesic segments with external angles $\theta_0, \ldots, \theta_k$, gives the formula

$$\int_R \left(1 + \frac{n-1}{r^2}\right) dxdr = 2\pi - \sum_{i=0}^{k} \theta_i. \tag{8}$$

It follows that such a region cannot contain too much Euclidean area, and if the region is close to the x-axis, then it must enclose small Euclidean area. In Section 5 we use the Gauss-Bonnet formula to establish convergence results for certain families of solutions to (3).

3. Graphical geodesic segments

Let $\gamma : I \to \mathbb{H}$ be a solution to (3), and let $\Gamma = \gamma(I)$ be its image. We begin this section by introducing terminology and notation for a subset of Γ that may be written as the graph of a function over the x-axis. Recall that Γ is the image of a geodesic for the conformal metric g_{Ang}. We say that $\Lambda \subset \Gamma$ is a *graphical geodesic segment* if $\Lambda = \{(x, u(x)) | x \in (a, b)\}$, where $u : (a, b) \to (0, \infty)$ is a solution to (4). In the case where $u(x)$ is a maximally extended solution on (a, b), we say that Λ is a *maximally extended graphical geodesic segment*.

Our construction of immersed self-shrinkers follows from the study of maximally extended graphical geodesic segments. We define $\underline{\Lambda}$ to be the set of non-linear maximally extended graphical geodesic segments. A consideration of (3) shows that the only linear solutions to (3) correspond to the plane $\mathcal{P}$ and the cylinder $\mathcal{C}$. It follows that $\underline{\Lambda}$ is the set of graphical geodesic segments $\Lambda \neq \mathcal{C}$ that can be written as the graph of a maximally extended solution to (4).

For a non-linear solution $\gamma : [0, s_r) \to \mathbb{H}$ to (3), we describe an ordered decomposition of $\gamma([0, s_r))$ using elements of $\underline{\Lambda}$ determined by the parametrization of $\gamma(s)$:

(Step 0) Extend γ to be a maximally extended solution $\gamma : (s_\ell, s_r) \to \mathbb{H}$. For small values of $s > 0$, the image of $\gamma(s)$ may be written as a graph of a solution $u(x)$ to (4). Since we're now assuming γ is maximally extended, we also assume that $u : (a, b) \to (0, \infty)$ is a maximally extended solution to (4). We define $\Lambda_0(\Gamma) \in \underline{\lambda}$ to be the graph of $u(x)$.

(Step 1) The parametrization of $\gamma(s)$ determines whether $\Lambda_0(\gamma)$ is traversed from 'left to right' or from 'right to left'. Suppose it is traversed from 'left to right'. If $b < \infty$ and $u(b) > 0$ (see Lemma 8), then $\gamma(s)$ 'turns around' at the right end point $(b, u(b))$, and its image can be written as the graph of a maximally extended solution $v : (c, b) \to (0, \infty)$ to (4) with the

same right end point $(b, v(b)) = (b, u(b))$. In this case, we denote the graph of $v(x)$ by $\Lambda_1(\gamma)$. If either $b = \infty$ or $u(b) = 0$, then $\Lambda_1(\gamma)$ is not defined.
Still assuming $\Lambda_0(\gamma)$ is traversed from 'left to right', if $a > -\infty$ and $u(a) > 0$, then $\gamma(s)$ 'turns around' at the left end point $(a, u(a))$, and its image can be written as the graph of a maximally extended solution $w : (a, d) \to (0, \infty)$ to (4) with the same left end point $(a, w(a)) = (a, u(a))$. In this case, we denote the graph of $w(x)$ by $\Lambda_{-1}(\gamma)$. If either $a = -\infty$ or $u(a) = 0$, then $\Lambda_{-1}(\gamma)$ is not defined.
If $\Lambda_0(\gamma)$ is traversed from 'right to left', then the order is reversed. That is, $\Lambda_{-1}(\gamma)$ is the graph of $v(x)$ and $\Lambda_1(\gamma)$ is the graph of $w(x)$.

(Step k) In general, $\Lambda_k(\gamma), \Lambda_{-k}(\gamma) \in \underline{\Lambda}$, $i \in \mathbb{Z}^+$, are determined inductively by applying the process in Step 1 to $\Lambda_{k-1}(\gamma)$ and $\Lambda_{-(k-1)}(\gamma)$. This gives the possibly finite ordered decomposition determined by the parametrization of $\gamma(s)$:

$$\gamma((s_\ell, s_r)) = \cdots \cup \overline{\Lambda_{-1}(\gamma)} \cup \overline{\Lambda_0(\gamma)} \cup \overline{\Lambda_1(\gamma)} \cup \cdots ,$$

where $\overline{\Lambda_k(\gamma)}$ includes any end points of $\Lambda_k(\gamma)$. Here we say that the image of $\gamma(s)$ is the union of the graphical geodesic segments $\Lambda_k(\gamma)$.

To give a detailed description of the shape of a graphical geodesic segment, we need to identify the points where its Euclidean curvature vanishes. In Proposition 3 we show that the Euclidean curvature of a graphical geodesic segment $\Lambda \in \underline{\Lambda}$ vanishes at no more than two points. We define the *type* of a graphical geodesic segment $\Lambda \in \underline{\Lambda}(i)$ as follows: Writing Λ as the graph of a maximally extended solution $u : (a, b) \to (0, \infty)$ to (4), since u'' vanishes at no more than two points, we know that u'' has a fixed sign near b. We say that Λ is type $(i, +)$ if u'' vanishes at i points and u'' is positive near b, and we say that Λ is type $(i, -)$ if u'' vanishes at i points and u'' is negative near b. We note that there are no type $(2, -)$ graphical geodesic segments in $\underline{\Lambda}$. (See Figure 2 for sketches of the different types of graphical geodesic segments.)

3.1. **Half-entire graphs: Trumpets and quarter-spheres.** Here we introduce a subset of $\underline{\Lambda}$ whose elements will play an important part in the construction of complete self-shrinkers with rotational symmetry. We define an element in $\underline{\Lambda}$ to be a *half-entire graph* if it is the graph of a maximally extended non-linear solution to (4) that is not compactly contained in the upper half-plane $\mathbb{H} = \{(x, r) | x \in \mathbb{R}, r > 0\}$. We denote the set of half-entire graphs by $\underline{H}$.

In [22], the second author and Møller constructed a one parameter family of half-entire solutions to (4). They showed that for each $\sigma > 0$ and linear function $r_\sigma(x) = \sigma x$, there exists a unique (non-entire) solution $u_\sigma : (a_\sigma, \infty) \to (0, \infty)$ to (4) that is asymptotic to $r_\sigma(x)$ as $x \to \infty$. Moreover, the solution u_σ has with the following properties: $a_\sigma \in (-\infty, 0)$; $u_\sigma(0) < \sqrt{2(n-1)}$; and $u_\sigma > r_\sigma$, $0 < u_\sigma' < \sigma$, and $u_\sigma'' > 0$ on $[0, \infty)$. In addition, any solution to (4) defined on an interval (a, ∞) must either be a trumpet u_σ or the cylinder $u(x) \equiv \sqrt{2(n-1)}$. An immediate consequence of this last result is that the cylinder is the only entire

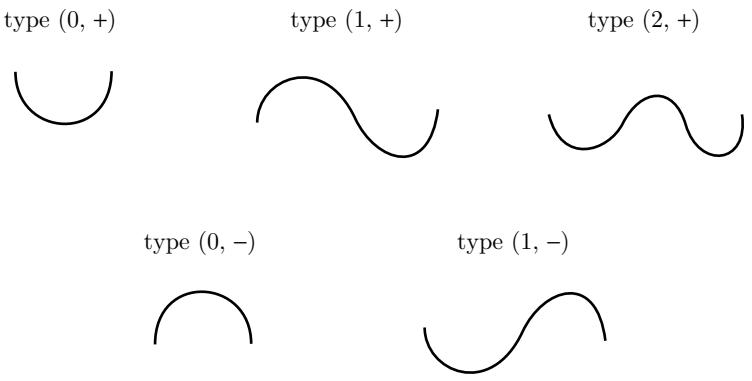

FIGURE 2. Sketches of the different types of graphical geodesic segments.

solution to (4). By symmetry there is a similar one parameter family of solutions u_σ for $\sigma < 0$. In this paper, we will refer to the graph of u_σ as a *trumpet*. We remark that the trumpets are the motivation for the terminology half-entire graph, as they come from graphs of half-entire solutions to (4).

Another one parameter family of elements in $\underline{\Lambda}$ comes from shooting orthogonally to the x-axis. Even though (3) is singular along the x-axis, there is a smooth one parameter family $Q[x_0]$ of solutions to the following initial value problem (see the Appendix of [10], or [4, Theorem 2.2]):

$$Q[x_0](0) = (x_0, 0), \quad Q[x_0]'(0) = (0, 1).$$

We note that $Q[\sqrt{2n}]$ and $Q[0]$ provide parametrizations for the sphere $\mathcal{S}$ and the plane $\mathcal{P}$, respectively. It was shown in [10] that there is $0 < x_1 < \sqrt{2n}$ so that $Q[x_1]$ is the profile curve of an immersed sphere self-shrinker.

The solutions $Q[x_0]$ defined above correspond to a family of half-entire graphs that exit through the x-axis, namely the graphical geodesic segments $\Lambda_0(Q[x_0])$. To be clear, the image of $Q[x_0](s)$, for small $s > 0$, may be written as a graph over the x-axis and $\Lambda_0(Q[x_0])$ is the maximally extended graphical geodesic segment corresponding to this graph. We refer to the graphical geodesic segment $\Lambda_0(Q[x_0])$ as a *quarter-sphere*.

Using the linearization of the rotational self-shrinker differential equation near the sphere, Huisken's theorem on mean-convex self-shrinkers, and a comparison result for solutions to (6), we can prove the following result.

Proposition 1. *Fix $x_0 \neq 0$, and set $Q = \Lambda_0(Q[x_0])$. Define $u = u_Q$ to be the solution of (4) so that the graph of u equals Q. Then $u(0) > \sqrt{2n}$ and $u'(0) < 0$ when $0 < x_0 < \sqrt{2n}$, and $u(0) < \sqrt{2n}$ and $u'(0) > 0$ when $x_0 > \sqrt{2n}$.*

Proof. The proof of this proposition follows from the results in Appendix A and Appendix B. Using the linearization of the rotational self-shrinker differential equation near the sphere and Huisken's theorem, we have $u'(0) < 0$ when $0 < x_0 < \sqrt{2n}$, and $u'(0) > 0$ when $x_0 > \sqrt{2n}$ (see Proposition 13 in Appendix B). Using the comparison results from Appendix A (see Proposition 11 and Proposition 12), we know that Q intersects the sphere exactly once in the first quadrant, so that $u(0) > \sqrt{2n}$ when $0 < x_0 < \sqrt{2n}$, and $u(0) < \sqrt{2n}$ when $x_0 > \sqrt{2n}$. □

In the following proposition, we observe that the trumpets and quarter-spheres account for all of the half-entire graphs. The proof of this proposition follows from a result of [22] and several results in Section 3.2.

Proposition 2. *The set $\underline{H}$ of half-entire graphs is the set of trumpets and quarter-spheres.*

Proof. Let $u : (a, b) \to (0, \infty)$ be a non-linear solution to (3) whose graph is not compactly contained in the upper half-plane. In [22] it is shown that if either $a = -\infty$ or $b = \infty$, then the graph of u is a trumpet. So, we consider the case where both a and b are finite. In this case, it follows from Lemma 8 that u is bounded above. Using Proposition 5 and Lemma 7, we deduce from equation (3) that the graph of u must be a quarter-sphere. □

Finally, we introduce additional terminology for the previously defined half-entire graphs:

> *Inner quarter-spheres:* The set $\underline{I}^+$ of inner quarter-spheres in the first quadrant is the collection of maximally extended graphical geodesic segments of the form $I_x := \Lambda_0(Q[x])$, for $0 < x < \sqrt{2n}$. Each $I \in \underline{I}^+$ intersects the r-axis above the sphere with negative slope.
>
> *Outer quarter-spheres:* The set $\underline{O}^+$ of outer quarter-spheres in the first quadrant is the collection of maximally extended graphical geodesic segments of the form $O_x := \Lambda_0(Q[x])$, for $x > \sqrt{2n}$. Each $O \in \underline{O}^+$ intersects the r-axis below the sphere with positive slope.
>
> *Trumpets:* The set $\underline{T}^+$ of trumpets in the first quadrant is the collection of the graphs of u_σ, where u_σ are the trumpets from [22] and $\sigma > 0$. Each $T \in \underline{T}^+$ intersects the r-axis below the cylinder with a positive slope.

The sets of half-entire graphs in the second quadrant: $\underline{I}^-$, $\underline{O}^-$, and $\underline{T}^-$ are defined similarly. We also introduce the sets:

$$\underline{I} = \underline{I}^+ \cup \underline{I}^- \cup \{\mathcal{S}\}, \qquad \underline{O} = \underline{O}^+ \cup \underline{O}^- \cup \{\mathcal{S}\}, \qquad \underline{T} = \underline{T}^+ \cup \underline{T}^-.$$

3.2. **Structure of graphical geodesic segments.** In this section we show if $u(x)$ is a non-linear solution to (4), then $u(x)$ has at most one local maximum, and consequently $u''(x)$ vanishes at no more than two points.

Proposition 3. *Let $\Lambda \in \underline{\Lambda}$ be a maximally extended graphical geodesic segment. Then the Euclidean curvature of Λ vanishes at no more than two points. Moreover, the only maximally extended graphical geodesic segments in $\underline{\Lambda}(2)$ are type $(2, +)$.*

The proposition is proved by carefully studying properties of solutions to (4) and (6). The proof is divided into two main parts. In the first part, we describe the behavior of solutions to (4) on one side of a local minimum. In the second part, we show that 0 is contained in the domain of a maximally extended solution to (4).

It follows from the analysis in Section 2 combined with the proof of Proposition 3 that a maximally extended graphical geodesic segment in $\underline{\Lambda}$ has one of the shapes sketched in Figure 2. In fact, we will prove the following structure theorem for maximally extended graphical geodesic segments.

Theorem 2 (Structure of graphical geodesic segments)**.** *Let Λ be a maximally extended graphical geodesic segment in $\underline{\Lambda}$, and let $u : (a, b) \to (0, \infty)$ be the nonlinear maximally extended solution to (4) whose graph is Λ. Then u'' vanishes at no more than two points; the zeros of u'' are disjoint from and separated by the zeros of u'; when u is increasing (decreasing) its concavity can only change from concave up to concave down (concave down to concave up); and at a local maximum (minimum) u is greater than (less than) $\sqrt{2(n-1)}$. In addition, if Λ is a trumpet, then $u'' > 0$ and Λ is type $(0, +)$; if Λ is not a trumpet, then $-\infty < a < b < \infty$ and u is bounded above; and there are no type $(2, -)$ maximally extended graphical geodesic segments.*

3.2.1. *Behavior of graphical geodesic segments at a local minimum.* We begin the proof of Proposition 3 by proving the following result.

Proposition 4. *Let $u : [x_0, b) \to (0, \infty)$ be a solution to (4) with*

$$u(x_0) < \sqrt{2(n-1)}, \quad u'(x_0) = 0,$$

where $x_0 \geq 0$. Then $u''(x) > 0$ for $x \in [x_0, b)$.

First, we show that a solution to (4) must be convex when it intersects the r-axis perpendicularly below the cylinder. This is the $x_0 = 0$ case in Proposition 4.

Lemma 5. *Let $u : [0, b) \to (0, \infty)$ be a solution to (4) satisfying*

$$u(0) < \sqrt{2(n-1)}, \quad u'(0) = 0.$$

Then $u''(x) > 0$ for $x \in [0, b)$.

Proof. Let $u_t : (a_t, b_t) \to (0, \infty)$ be the maximally extended solution to (4) satisfying $u_t(0) = t$, $u_t'(0) = 0$. When $t < \sqrt{2(n-1)}$, we have $u''(0) > 0$, and if u_t is not strictly convex, then there must be a first point $c_t > 0$ so that

$$u_t(c_t) = \sqrt{2(n-1)}.$$

This follows from equation (4) since $u_t''(x) > 0$ when $x > 0$, $u_t'(x) > 0$, and $u_t(x) < \sqrt{2(n-1)}$.

Examining equation (4) when $x = c_t$, we conclude that $u_t'' > 0$ on the closed interval $[0, c_t]$. Applying Lemma 3 to u_t written as a graph over the r-axis, shows that c_t cannot exist when $t < m_1$. Therefore, for small $t > 0$, we have $u_t'' > 0$ on $[0, b_t)$.

We will use continuity to show that $u_t'' > 0$ on $[0, b_t)$ for all $0 < t < \sqrt{2(n-1)}$. This requires three steps. The first step (non-empty) is to show the statement is true when $t > 0$ is small. This was done in the previous paragraph. The second step (open) is to show if the statement holds at t_0, then it also hold for nearby values of t. The third step (closed) is to show if the property holds for all t less than t_0, then it also holds at t_0.

To see that the second step holds, let $0 < t_0 < \sqrt{2(n-1)}$, and suppose u_{t_0} is strictly convex on $[0, b_{t_0})$. Then we know from Lemma 4 that the point $(b_{t_0}, u_{t_0}(b_{t_0}))$ is a finite point in the upper half-plane (here $u_{t_0}(b_{t_0})$ is the finite limit of $u_{t_0}(x)$ as $x \to b_{t_0}^-$). Moreover, the graph of u_{t_0} may be continued as a solution to (3) that is convex as a Euclidean curve and turns around at this point. Furthermore, by continuity any nearby solution to (3) will exhibit the same behavior. In particular, for t close to t_0, the solution u_t will be strictly convex.

To see that the third step holds, fix $t_0 \in (0, \sqrt{2(n-1)})$, and suppose $u_t'' > 0$ on $[0, b_t)$ for all $0 < t < t_0$. By continuity, we must have $u_{t_0}'' \geq 0$ on $[0, b_{t_0})$. Using equation (5), we conclude that u_{t_0} is strictly convex. This completes the proof of the lemma. □

Proof of Proposition 4. Fix $x_0 > 0$ and $r_0 < \sqrt{2(n-1)}$, and consider the family of shooting problems for (4): $u_t(t) = r_0$, $u_t'(t) = 0$, where $t \in [0, x_0]$. We want to show the solution $u_t : [t, b_t) \to (0, \infty)$ to (4) is strictly convex on $[t, b_t)$. The proof is similar to the proof of Lemma 5, so we only provide a sketch. Note that x_0 and r_0 are fixed, so the parameter t that is varying is the initial x-coordinate. It follows from Lemma 5, that u_0 is strictly convex on $[0, b_0)$. This is the first step of the continuity argument. As the parameter t varies from 0 to x_0, the second and third steps of the continuity argument are similar to their analogues in the proof of Lemma 5. □

3.2.2. *Maximally extended graphical geodesic segments intersect the r-axis.* Now we are ready to finish the proof of Proposition 3. In terms of solutions to (4), we prove the following result.

Proposition 5. *Let $u : (a, b) \to (0, \infty)$ be a non-linear maximally extended solution to* (4)*. Then $a < 0 < b$. Moreover, u'' can only vanish at two points.*

We first prove the following fact which is needed in the proof of Proposition 5.

Lemma 6. *Let u be a solution to* (4) *defined on a finite interval (x_1, x_2). If $u' < 0$ and $u'' > 0$ on (x_1, x_2), then $\lim_{x \to x_2} u(x) > 0$.*

Proof. It is sufficient to show that a solution $f(r)$ to (6) defined on (r_1, r_2) with $f \leq M$, $f' < 0$, and $f'' > 0$ satisfies $r_1 > 0$. Let $\alpha(r) = -(\pi/2 + \arctan f'(r))$ so that $\alpha(r) \in (-\pi/2, 0)$ and

$$\frac{d}{dr}(\log \cos \alpha(r)) = \frac{r}{2} - \frac{n-1}{r} - \frac{f(r)}{2f'(r)} \leq \frac{r}{2} - \frac{n-1}{r} + \frac{M}{2(-f'(r_2))}.$$

Integrating from r_1 to r_2,

$$\log\left(\frac{\cos \alpha(r_2)}{\cos \alpha(r_1)}\right) \leq \frac{(r_2)^2}{4} + (n-1)\log\left(\frac{r_1}{r_2}\right) + \frac{Mr_2}{2(-f'(r_2))}.$$

Therefore,

$$r_1 \geq r_2 \left[\cos \alpha(r_2) e^{-\frac{(r_2)^2}{4} + \frac{Mr_2}{2f'(r_2)}}\right]^{1/(n-1)}.$$

□

Now, we are ready to prove Proposition 5.

Proof of Proposition 5. Let $u : (a, b) \to (0, \infty)$ be a non-linear maximally extended solution to (4). Since $u(-x)$ is also a solution to (4), we may assume without loss of generality that $a < 0$.

It follows from Proposition 4 that u has at most two local minimum points (one in each quadrant). This coupled with Lemma 1 shows that $u''(x)$ vanishes at no more than two points, and u has at most one local maximum. Hence there are no type $(2, -)$ graphical geodesic segments. As a maximally extended solution to (4), these restrictions show that $u(x)$ is monotone and convex as $x \to b^-$.

Now, we can show that $b > 0$. We know that u'' does not vanish in a neighborhood of b. Examining equation (4) and using Lemma 6, we see that $u'(x)$ and $u''(x)$ must have the same sign when x is near b. If $\lim_{x\to b} u(x) \in (0,\infty)$, then $\lim_{x\to b} |u'(x)| = \infty$ (since u is maximally extended), and it follows from (4) that $b \geq 0$. In fact, $b > 0$, since the graph of u cannot be tangent to the plane $\mathcal{P}$. If $\lim_{x\to b} u(x)$ is 0 (or ∞), then u' and u'' are both negative (or both positive), and the term $\left(\frac{n-1}{u} - \frac{u}{2}\right)$ has the correct sign to force $b > 0$. □

We make note of a result used during the proof of Proposition 5.

Lemma 7. *Let $u : (a,b) \to \mathbb{R}$ be a maximally extended non-degenerate solution to (4). Then u' and u'' do not vanish in a neighborhood of b (or a). Moreover, u' and u'' have the same sign (have different signs) in this neighborhood.*

Proof. The lemma is true when $b = \infty$ by [22, Theorem 3]. We assume that $b < \infty$. We also assume, as in the proof of Proposition 5, that u'' does not vanish in a neighborhood of b. Using Lemma 6, we know that u' and u'' must have the same sign when $u(x) \to 0$ as $x \to b^-$. If $u(x) \to \infty$ as $x \to b^-$(which in fact does not happen when $b < \infty$), then we have $u'(x), u''(x) \to \infty$ as $x \to b$. Finally, when $0 < \lim_{x\to b} u(x) < \infty$, it follows that $\lim_{x\to b} |u'(x)| = \infty$, and u' and u'' have the same sign near b. □

As a consequence of Lemma 7, we have the slight improvement of Lemma 4.

Lemma 8. *Let $u : (a,b) \to \mathbb{R}$ be a maximally extended solution to (4). If b (or a) is finite, then $\lim_{x\to b} u(x) < \infty$ (or $\lim_{x\to a} u(x) < \infty$).*

Proof. We know from Lemma 7 that the $u'(x)$ and $u''(x)$ have the same sign (and do not vanish) as x approaches b. When u' and u'' are both negative near b, so that u is decreasing, the lemma holds. When u' and u'' are both positive near b, the proof follows as in the proof of Lemma 4 □

Next, we show that a solution to (4) which intersects the r-axis below the cylinder with negative slope is convex in the first quadrant.

Lemma 9. *Let $u : [0,b) \to (0,\infty)$ be a solution to (4) satisfying*

$$u(0) < \sqrt{2(n-1)}, \quad u'(0) < 0.$$

Then $u''(x) > 0$ for $x \in [0,b)$.

Proof. We assume that u is maximally extended at b. Since $u(0) < \sqrt{2(n-1)}$ and $u'(0) < 0$, we know that $b < \infty$, and $u''(x) > 0$ as long as $u' < 0$ on $[0,x)$. It then follows (from Lemma 7) that u has a minimum somewhere on $[0,b)$. Applying Proposition 4 to the first minimum on $[0,b)$ proves the lemma. □

Slightly adapting the previous proof of Lemma 9 we can show that a solution to (4) which intersects the r-axis between the cylinder and the sphere with negative slope has an inflection point in the first quadrant.

Lemma 10. *Let $u : [0,b) \to (0,\infty)$ be a solution to (4), maximally extended at b, satisfying*

$$\sqrt{2(n-1)} \leq u(0) \leq \sqrt{2n}, \quad u'(0) < 0.$$

Then there is a point $x_0 \in [0,b)$ so that $u''(x) \leq 0$ for $x \in [0,x_0]$, and $u''(x) > 0$ for $x \in (x_0,b)$. Furthermore, there is a point $x_1 > x_0$ for which $u'(x_1) = 0$.

Proof. We consider the following family of shooting problems: For $t \in (0, u(0)]$, let $u_t : [0, b_t) \to (0, \infty)$ be the solution to (4) with $u_t(0) = t$ and $u_t'(0) = u'(0)$. We assume that u_t is maximally extended at b_t, and we will use the facts that $b_t < \infty$ and $\lim_{x \to b_t} u_t(x) < \infty$, which follow from [22, Theorem 3] and Lemma 8.

When $t < \sqrt{2(n-1)}$, we know (from the proof of Lemma 9) that u_t has a unique local minimum at a point $x_1^t \in (0, b_t)$ (the uniqueness follows from Proposition 4). We claim that this property is true for all $t \leq u(0)$. Suppose to the contrary that u_{t_*} does not have a local minimum in $(0, b_{t_*})$ for some first $t_* \leq u(0)$. Then, as t increases to t_*, the points $p_t = (x_1^t, u_t(x_1^t))$ must leave the first quadrant of the upper half-plane. Since $u_t'(0) = u'(0) < 0$ and $u_t(0) \leq u(0)$, we know that the points p_t are bounded away from the r-axis. By continuity, since $b_{t_*} < \infty$, we know that x_1^t is bounded above when t is less than and close to t_*. We also know that $u_t(x_1^t) \leq u(0)$ when $t < t_*$. Finally, since $u_{t_*}(0) \leq \sqrt{2n}$ and $u_{t_*}'(0) < 0$ we know from Proposition 1 that the graph of u_{t_*} is not a quarter-sphere and by continuity the points p_t are bounded away from the x-axis. Therefore, the points p_t remain inside a compact subset of the first quadrant, which is a contradiction. We conclude that u_t has a unique local minimum at a point $x_1^t \in (0, b_t)$ for all $t \leq u(0)$.

Now, we can describe the behavior of u_t when $\sqrt{2(n-1)} \leq t \leq u(0)$. We know that u_t has a local minimum at x_1^t, and applying Proposition 4 we have $u_t''(x) > 0$ for $x \geq x_1^t$. Since $u_t'(0) < 0$, we have $u_t''(0) \leq 0$. Now, we know that $u_t''(x)$ can vanish at most once when $x \geq 0$, so using $u_t''(x_1^t) > 0$, we see that $u_t''(x_0^t) = 0$ at some point $x_0^t \in [0, x_1^t)$ and $u_t''(x) > 0$ for $x \in (x_0^t, b_t)$. □

Finally, we are ready to prove Proposition 3. The following proof also establishes Theorem 2.

Proof of Proposition 3. Let $\Lambda \in \underline{\Lambda}$ be a maximally extended graphical geodesic segment, and let $u : (a, b) \to (0, \infty)$ be the maximally extended (non-linear) solution to (4) whose graph is Λ. It follows from Proposition 5 that $0 \in (a, b)$ and u'' vanishes at no more than two points. We will show that Λ has one of the shapes sketched in Figure 2.

Case 0. If u'' does not vanish, then u is convex and Λ is type $(0, +)$ or type $(0, -)$ depending on the sign of u''. We note that the trumpets are convex. This follows from [22, Theorem 3] and Lemma 9.

Case 1. If u'' vanishes at exactly one point $x_0 \in (a, b)$, then by (4) and the uniqueness of the constant solution $r \equiv \sqrt{2(n-1)}$, we know that $u'(x_0) \neq 0$. By the symmetry of (4) with respect to reflections across the r-axis, we may assume that $u'(x_0) > 0$. It follows from Section 2.1 that $u''(x) < 0$ for $x \in (x_0, b)$ and $u''(x) > 0$ for $x \in (a, x_0)$. Applying Lemma 7 and noting that Λ is not a trumpet in this case, we see that there are points x_1 and x_2 with $a < x_1 < x_0 < x_2 < b$ so that u has a local maximum at x_2 and a local minimum at x_1. It follows from convexity that Λ has the shape of the type $(1, -)$ curve sketched in Figure 2.

Case 2. If u'' vanishes at two points in (a, b), say $x_1 < x_2$, then it follows from Lemma 1 that there is a point $x_0 \in (x_1, x_2)$ so that $u'(x_0) = 0$. By the symmetry of (4) with respect to reflections across the r-axis, we may assume that $x_0 \geq 0$. Then, an application of Proposition 4 shows that u has a local maximum at x_0. Notice that u is convex on the intervals (a, x_1) and (x_2, b), and a repeat of the analysis from Case 1 can be used to describe the behavior of u on these intervals.

It follows that Λ has the shape of the type $(2,+)$ curve sketched in Figure 2. Hence there are no type $(2,-)$ curves. □

3.3. **The types of the half-entire graphs.** In this section we classify the half-entire graphs into their different types $(i,\pm)$.

Proposition 6 (Half-entire graph types)**.** *The elements of $\underline{I}^+$ are type $(0,-)$, the elements of $\underline{O}^+$ are type $(1,-)$, and the elements of $\underline{T}^+$ are type $(0,+)$.*

Proof. We consider the half-entire graphs in the first quadrant. It was shown in [10, Proposition 4.12] that $\Lambda_0(Q[x_0])$ is type $(0,-)$ for small x_0. In fact, it was shown in [10] that $\Lambda_0(Q[x_0])$ has a maximum in the second quadrant and a finite left end point for small $x_0 > 0$. Arguing by continuity and using Huisken's theorem for mean-convex self-shrinkers, we see that this property persists for $0 < x_0 < \sqrt{2n}$. Therefore, the curves in $\underline{I}^+$ are type $(0,-)$. When $x_0 > \sqrt{2n}$, we know that $\Lambda_0(Q[x_0])$ intersects the r-axis below the sphere with positive slope, and it follows from Lemma 9 and Lemma 10 that $\Lambda_0(Q[x_0])$ is type $(1,-)$. Therefore, the curves in $\underline{O}^+$ are type $(1,-)$. Finally, it follows from Lemma 9 that the curves in $\underline{T}^+$ are type $(0,+)$ since they intersect the r-axis below the cylinder with positive slope. □

4. The shooting problems

Our construction of immersed self-shrinkers involves the study of two shooting problems for solutions to (3). In one of the shooting problems, we shoot perpendicularly from the x-axis, and in the other shooting problem, we shoot perpendicularly from the r-axis. In both cases, the goal is essentially to find a solution γ to (3) so that the graphical geodesic segment $\Lambda_k(\gamma)$ is a half-entire graph, for some $k > 0$. Such a solution is then the profile curve for a complete self-shrinker with rotational symmetry. In addition, by the symmetry of equation (3) with respect to reflections about the r-axis, if $\Lambda_k(\gamma)$ intersects the r-axis perpendicularly, for some $k > 0$, then γ is also the profile curve for a complete self-shrinker.

First, we consider the problem of shooting perpendicularly to the x-axis. This problem was introduced in Section 3.1. For $t \in \mathbb{R}$, we let $Q[t]$ be the solution to (3) satisfying

$$Q[t](0) = (t,0), \quad Q[t]'(0) = (0,1).$$

We note the solutions $Q[t]$ are well-defined and depend smoothly on the parameter t (see the Appendix of [10], or [4, Theorem 2.2]). When $t \in (0,\sqrt{2n})$, the solutions $Q[t]$ intersect the x-axis perpendicularly in the first quadrant, and $\Lambda_0(Q[t])$ is type $(0,-)$.

Next, we consider the problem of shooting perpendicularly to the r-axis. To introduce this shooting problem, we note that an arclength parametrized curve $\gamma(s) = (x(s), r(s))$ is a solution to (3) if and only if the angle $\alpha(s)$ solves

$$\dot{\alpha}(s) = \frac{x(s)}{2}\sin\alpha(s) + \left(\frac{n-1}{r(s)} - \frac{r(s)}{2}\right)\cos\alpha(s), \tag{9}$$

where $\dot{x}(s) = \cos\alpha(s)$ and $\dot{r}(s) = \sin\alpha(s)$. For $(x_0, r_0) \in \mathbb{H}$ and $\alpha_0 \in \mathbb{R}$, we let $\gamma[x_0, r_0, \alpha_0]$ denote the unique solution to (9) satisfying

$$\gamma[x_0, r_0, \alpha_0](0) = (x_0, r_0), \quad \dot{\gamma}[x_0, r_0, \alpha_0](0) = (\cos(\alpha_0), \sin(\alpha_0)). \tag{10}$$

The second shooting problem we consider is the one parameter family of solutions $\gamma[0,t,0]$, for $t > 0$. We note that these solutions initially intersect the r-axis perpendicularly, and immediately travel into the first quadrant. When $0 < t < \sqrt{2(n-1)}$, we also note that $\Lambda_0(\gamma[0,t,0])$ is type $(0,+)$.

5. Applications of the Gauss-Bonnet formula

In this section we use the Gauss-Bonnet formula (8) to prove some convergence results for solutions to (3) and the geodesics they parametrize in the upper half-plane $\mathbb{H}$ with the conformal metric g_{Ang}. We begin with an observation about continuous families of graphical geodesic segments in $\underline{\Lambda}$.

Lemma 11. *For $t \in [t_1, t_2]$, let $\Lambda_t \in \underline{\Lambda}$ be a family of maximally extended graphical geodesic segments, given as the graphs of a family of solutions $u_t : (a_t, b_t) \to (0, \infty)$ to (4). We assume the family of graphical geodesic segments is continuous in the sense that $u_t(0)$ and $u_t'(0)$ vary continuously. Now, suppose the right end points $p_t = (b_t, u_t(b_t))$ are contained in a compact subset of the upper half-plane. Also, suppose Λ_{t_1} and Λ_{t_2} have different types and neither one is a half-entire graph. Then there exists $t_0 \in (t_1, t_2)$ so that Λ_{t_0} is a half-entire graph and its right end point is contained in a compact subset of the upper half-plane.*

Proof. Since Λ_{t_1} is not a half-entire graph, it is contained in a compact subset of $\mathbb{H}$. By continuity, for t close to and greater than t_1, we know that Λ_t has the same type as Λ_{t_1} and it is not a half-entire graph. Let t_0 be the first t greater than t_1 so that one (or both) of these properties fails to hold: either Λ_{t_0} is a different type than Λ_{t_1} or Λ_{t_0} is a half-entire graph. Since Λ_{t_2} is a different type from Λ_{t_1}, we know $t_0 \leq t_2$. In fact, since Λ_{t_2} is contained in a compact subset of $\mathbb{H}$, it follows from continuity that $t_0 < t_2$. Again by continuity, we see that the graphical geodesic segments Λ_t do not remain in a compact set as $t \to t_0^-$. It follows that Λ_{t_0} is a half-entire, and by assumption its right end point is contained in a compact subset of $\mathbb{H}$. □

Next, we introduce a notion of convergence for elements in $\underline{\Lambda}$. Let $\Lambda_t \in \underline{\Lambda}$ be a family of graphical geodesic segments, given as the graphs of a family of solutions $u_t : (a_t, b_t) \to (0, \infty)$ to (4). We say the family of graphical geodesic segments is continuous if $u_t(0)$ and $u_t'(0)$ vary continuously. For a graphical geodesic segment Λ_∞, which is given as the graph of a maximally extended solution u_∞, we say that $\Lambda_t \to \Lambda_\infty$ if $u_t(0)$ and $u_t'(0)$ converge to $u_\infty(0)$ and $u_\infty'(0)$, respectively.

The remainder of this section is dedicated to proving the following proposition and its corollary on the convergence of graphical geodesic segments to half-entire graphs.

Proposition 7. *Let $\gamma[t] : [0, s_t) \to \mathbb{H}$ be a continuous family of solutions to one of the two shooting problems from Section 4 or possibly a shooting problem from the r-axis with non-zero initial angle. For some range of t, say $t \in [t_1, t_\infty)$, suppose that $\Lambda_{k+1}(\gamma[t])$ exists. Let p_t be the point determined by the parametrization of $\gamma[t]$ where $\Lambda_{k-1}(\gamma[t])$ meets $\Lambda_k(\gamma[t])$, and suppose that p_t is contained in some compact subset of $\mathbb{H}$, for $t \in [t_1, t_\infty)$. If $\Lambda_k(\gamma[t]) \to \Lambda_\infty$ as $t \to t_\infty$, where Λ_∞ is a half-entire graph, then $\Lambda_{k+1}(\gamma[t]) \to \Lambda_\infty$ as $t \to t_\infty$. The conclusion also holds when Λ_∞ is the cylinder.*

Several convergence results can be established using Proposition 7. For instance, the limit of type $(1,-)$ graphical geodesic segments whose right end points remain bounded away from the r-axis in a compact subset of $\mathbb{H}$, must either be a type $(1,-)$ or a type $(0,-)$ graphical geodesic segment. In particular, if these graphical geodesic segments converge to a half-entire graph, then it must be in $\underline{I}^-$. We collect some of these results in the following corollary.

Corollary 1. *Let Λ_t be a family of graphical geodesic segments in $\underline{\Lambda}$ whose right end points p_t remain bounded away from the r-axis in a compact subset of $\mathbb{H}$. If $p_t \to p_\infty$, then there exists $\Lambda_\infty \in \underline{\Lambda}$ so that $\Lambda_t \to \Lambda_\infty$. Moreover, if Λ_∞ is a half-entire graph, then the following statements hold:*

1. *If Λ_t are type $(0,+)$, then Λ_∞ is in $\underline{T}^-$.*
2. *If Λ_t are type $(0,-)$, then Λ_∞ is in $\underline{I}^-$.*
3. *If Λ_t are type $(1,+)$, then Λ_∞ is in $\underline{O}^-$ or $\underline{T}^-$.*
4. *If Λ_t are type $(1,-)$, then Λ_∞ is in $\underline{I}^-$.*
5. *If Λ_t are type $(2,+)$, then Λ_∞ is in $\underline{O}^-$.*

We begin the proof of Proposition 7 with a lemma that describes the shape of a solution $u(x)$ to (4) when $u(0)$ is small or large.

Lemma 12. *Let m_1 and M_1 be the constants defined in* Lemma 3 *and* Lemma 2. *If $u : (a,b) \to (0,\infty)$ is a maximally extended solution to* (4)*, then*

1. *If $u(0) < m_1$, then the graph of u is in $\underline{\Lambda}(0,+)$.*
2. *If $u(0) > M_1$, then the graph of u is in $\underline{\Lambda}(0,-)$.*

Moreover, $a, b \to 0$ as $u(0) \to 0$ or $u(0) \to \infty$.

Proof. First, we treat the case where $u(0) < m_1$. If $u'(0) < 0$, then it follows from Lemma 9 that $u''(x) > 0$ for $x \geq 0$. When $u'(0) \geq 0$, it follows from (4) that $u''(x) > 0$ for $x \geq 0$ as long as $u < \sqrt{2(n-1)}$ on $[0,x]$. In both cases, we observe that a portion of the geodesic $(x, u(x))$ may be written as a graph over the r-axis: $(f(r), r)$, where f is a solution of (6). We claim that $u < \sqrt{2(n-1)}$ on $[0,b)$. To see this, suppose to the contrary that $u(x) \geq \sqrt{2(n-1)}$ for some $x > 0$. Then we may choose f so that $f(r) > 0$, $f'(r) > 0$, and $f''(r) < 0$ when $m_1 \leq r \leq \sqrt{2(n-1)}$. Applying Lemma 3 shows that this is impossible, and therefore $u < \sqrt{2(n-1)}$ on $[0,b)$. In particular, we have $u'' > 0$ on $[0,b)$.

Now, we estimate b in terms of $u(0)$. If, say, $u(b) \leq 3u(0)$, then $u(x) \leq 3u(0)$ on $[0,b)$, and we can write equation (4) as

$$\frac{d}{dx}\left(\arctan u'\right) = \frac{xu' - u}{2} + \frac{n-1}{u} \geq -\frac{u(0)}{2} + \frac{n-1}{3u(0)},$$

where we have used $xu' - u$ is increasing on $(0,b)$. Integrating from 0 to b, we have

$$\pi \geq \left(\frac{n-1}{3u(0)} - \frac{u(0)}{2}\right) b,$$

and thus $b \to 0$ as $u(0) \to 0$. In general, if $u(b) = Au(0)$, where $A > 1$, then

$$\pi \geq \left(\frac{n-1}{Au(0)} - \frac{u(0)}{2}\right) b. \tag{11}$$

Notice that the Euclidean triangle T with vertices $(0,u(0))$, $(0,u(b))$, and $(b,u(b))$ is contained in a simple, compact region R bounded by the geodesic corresponding to u and possibly the r-axis. Here the boundary of R is the piecewise smooth union of geodesic segments with at most two external angles. Applying the Gauss-Bonnet formula (8) to R, we have

$$4\pi \geq \int_R \frac{n-1}{r^2} dxdr \geq \int_T \frac{n-1}{r^2} dxdr = \frac{(n-1)b}{(A-1)u(0)} \left[\log A + \frac{1}{A} - 1\right].$$

If A is sufficiently large, so that

$$\frac{1}{A-1}\left[\log A + \frac{1}{A} - 1\right] \geq \frac{\log A}{2A},$$

then

$$4\pi \geq \frac{(n-1)b\log A}{2Au(0)} = \frac{(n-1)b\log A}{2u(b)} \geq \frac{(n-1)b\log A}{2\sqrt{2(n-1)}} = \frac{\sqrt{n-1}}{2\sqrt{2}}\, b\log A. \tag{12}$$

It follows that $b \to 0$ as $u(0) \to 0$: Fix $\varepsilon > 0$, and choose $u(0) < \varepsilon e^{-1/\varepsilon}$. If $A < e^{1/\varepsilon}$, then $Au(0) < \varepsilon$ and (11) implies $b \lesssim \varepsilon$. If $A \geq e^{1/\varepsilon}$, then $\log A \geq 1/\varepsilon$ and (12) implies $b \lesssim \varepsilon$.

Second, we treat the case where $u(0) > M_1$. Since $u(0) > \sqrt{2(n-1)}$, we know that $u''(0) < 0$ and $b < \infty$. When $u'(0) \leq 0$, it follows from (4) that $u''(x) < 0$ for $x \geq 0$ as long as $u > \sqrt{2(n-1)}$ on $[0,x]$. When $u'(0) > 0$, we can use Lemma 1 combined with Lemma 7 to conclude that the first zero of u' occurs before the first zero of u'', and it again follows from (4) that $u''(x) < 0$ as long as $u > \sqrt{2(n-1)}$ on $[0,x]$. Now, the decreasing portion of the geodesic $(x,u(x))$ can be written as a graph over the r-axis: $(f(r),r)$, where f is a solution to (6) and $f(r) > 0$ and $f'(r) \leq 0$ when $u(b) \leq r \leq M_1$. Applying Lemma 2 shows $u(b) > \sqrt{2(n-1)}$. In particular, we have $u'' < 0$ on $[0,b)$.

To estimate b in terms of $u(0)$, we note that the function f from the above paragraph is defined on $[\sqrt{2(n-1)}, M_1]$. Using the shape of the graph of u and equations (6) and (7) we know that $f > 0$ and $f'' < 0$ on $[\sqrt{2(n-1)}, M_1]$. It follows that the Euclidean triangle T with vertices $(0,u(0))$, $(0,\sqrt{2(n-1)})$, and $(b,u(b))$ is contained inside a simple, compact region R bounded by geodesic segments. For instance, we may choose R to be the region containing T that is bounded by the r-axis, the geodesic $r \equiv \sqrt{2(n-1)}$, and the geodesic corresponding to u. Applying the Gauss-Bonnet formula (8) to this region R (and using that T is contained inside R), we arrive at the inequality

$$5\pi \geq \int_T dxdr = [u(0) - \sqrt{2(n-1)}]b/2,$$

so that $b \to 0$ as $u(0) \to \infty$.

Finally, the same arguments apply to the left end point a. □

Next, we prove a lemma which restricts the domain of a solution to (4) that intersects the r-axis with steep negative slope.

Lemma 13. *Given $\varepsilon > 0$, there exists $L > 0$ so that: If u is a maximally extended solution to (4) defined on the interval (a,b) with $u'(0) \leq -L$, then $b \in (0,\varepsilon)$.*

Proof. Fix $\varepsilon > 0$. We will show there is $L > 0$ so that $b \lesssim \varepsilon$ when $u'(0) \leq -L$. By Lemma 12, there exist positive constants m and M so that $b < \varepsilon$ when $u(0) < m$ or $u(0) > M$, so we may assume that $m \leq u(0) \leq M$. There are two cases to consider, depending on the shape of u.

Case 1. $u'(0) \leq -L$ and $u'' < 0$ on $[0, b)$. Since $u(0) \leq M$, $u'(0) \leq -L$, and $u'' < 0$, we know that $x \leq M/L$ whenever $u(x)$ is defined (integrate $u' \leq -L$ from 0 to x). Therefore $b \leq M/L$, and we may choose $L > M/\varepsilon$.

Case 2. $u'(0) \leq -L$ and $u''(x) \geq 0$ for some $x \geq 0$. For large enough L (depending only on M and ε), using the continuity of the differential equation (6), we know there is a point $(c, u(c))$ so that $c < \varepsilon$ and $u(c) < \varepsilon$. By choosing $L > M/\varepsilon$, we may assume that $u''(c) > 0$ (see Case 1). Furthermore, by allowing for $c < 2\varepsilon$, we may assume $u'(c) \geq -1$. We work with $\varepsilon e^{-1/\varepsilon}$ in place of ε: We assume $c, u(c) < \varepsilon e^{-1/\varepsilon}$. Arguing as in the proof of Lemma 12, we write equation (4) as

$$\frac{d}{dx}\left(\arctan u'(x)\right) = \frac{xu'(x) - u(x)}{2} + \frac{n-1}{u(x)} \geq -\varepsilon e^{-1/\varepsilon} + \frac{n-1}{u(x)},$$

where we have used $xu(x)' - u(x)$ is increasing when $x \geq c$, along with the estimates on c, $u(c)$, and $u'(c)$. If $u(b) = Au(c)$, for some $A > 1$, then integrating from c to b, we have

$$\pi \geq \left(\frac{n-1}{Au(c)} - \varepsilon e^{-1/\varepsilon}\right)(b - c). \tag{13}$$

Now, the Euclidean triangle T with vertices $(c, u(c))$, $(c, u(b))$, and $(b, u(b))$ is contained in a simple compact region R bounded by the geodesic corresponding to u and possibly the r-axis. Here the boundary of R is the piecewise smooth union of geodesic segments with at most two external angles. Applying the Gauss-Bonnet formula (8) to the region R, we arrive at the inequality

$$4\pi \geq \int_T \frac{n-1}{r^2} dx dr = \frac{(n-1)(b-c)}{(A-1)u(c)}\left[\log A + \frac{1}{A} - 1\right],$$

so that (arguing as in Lemma 12)

$$4\pi \geq \frac{(n-1)(b-c)\log A}{2Au(c)} \geq \frac{(n-1)(b-c)\log A}{2\sqrt{2(n-1)}} > \frac{\sqrt{n-1}}{2\sqrt{2}}\left(b - \varepsilon e^{-1/\varepsilon}\right)\log A, \tag{14}$$

when A is sufficiently large. If $A < e^{1/\varepsilon}$, then $Au(c) < \varepsilon$ and (13) implies $b \lesssim \varepsilon$. If $A \geq e^{1/\varepsilon}$, then $\log A \geq 1/\varepsilon$ and (14) implies $b \lesssim \varepsilon$. If $u(b) \leq u(c)$, then

$$\pi \geq \left(\frac{n-1}{u(c)} - \varepsilon e^{-1/\varepsilon}\right)(b - c),$$

and we also have $b \lesssim \varepsilon$. □

The following result will be used to restrict the domain of a solution to (4) that intersects the r-axis with steep positive slope.

Lemma 14. *Let u be a maximally extended solution to* (4) *defined on the interval (a, b). If u has a local maximum at $x_1 > 0$ and $u(x_1) > \max\{u(0), \sqrt{2(n-1)}\} + 2$, then $b < 2x_1$.*

Proof. This lemma follows from the proofs of [10, Claim 4.9] and [10, Lemma 4.10]. Those results show that $u(b) > u(x_1) - 2$, and $u(x_1 - s) \geq u(x_1 + s)$ when $s > 0$. Since $u(b) > u(x_1) - 2 > u(0)$ and $u'' < 0$ on $[0, b)$, we have $b < 2x_1$. For convenience, we include proofs of these two facts.

Part 1. $u(b) > u(x_1) - 2$. The graph $(x, u(x))$ for $x > x_1$ can be written as the graph $(f(r), r)$, where f is a solution to (6). Now $f > 0$ and $f' < 0$ in a neighborhood of $u(x_1)$ (when $f(r)$ is defined), and using equations (6) and (7), we also have $f'' < 0$ and $f''' < 0$. Assuming $f' < 0$, these inequalities hold when $r \geq \sqrt{2(n-1)}$. Repeatedly integrating $f''' < 0$ shows that $f(r_0) + f''(r_0)(r_1 - r_0)^2/2 > 0$, for $r_0 < r_1$. Then, using $f''(r_0) < -f(r_0)/2$ (which follows from (4) under the above assumptions), we have $[1 - (u(x_1) - r_0)^2/4] f(r_0)$. It follows that $f'(r) = 0$ for some $r > u(x_1) - 2$; hence $u(b) > u(x_1) - 2$.

Part 2. $u(x_1 - s) \geq u(x_1 + s)$ when $s > 0$. Since $u'(x_1) = 0$, using (6) and (7), we have

$$u'''(x_1) = \frac{x_1}{2}\left(\frac{n-1}{u(x_1)} - \frac{u(x_1)}{2}\right).$$

Let $\delta(s) = u(x_1 + s) - u(x_1 - s)$. Then $\delta(0) = \delta'(0) = \delta''(0) = 0$ and $\delta'''(0) = 2u'''(x_1) < 0$. It follows that $\delta(s) < 0$ for small $s > 0$. We will show that $\delta(s) < 0$ when $s > 0$. Let f be as in Part 1, and let g be the solution to (6) corresponding to the graph of $u(x)$ for $x \leq x_1$. We note that there exists $0 < t < s$ so that $u(x_1 + t) = u(x_1 - s)$ when $s > 0$ is small. Setting $h(r) = f(r) + g(r)$, we have $h(r) = 2x_1 + t - s < 2x_1$ so that $h(r) < 2x_1$ when $r < u(x_1)$ is close to $u(x_1)$. We claim that $h(r) < 2x_1$ for $r \in (u(b), u(x_1))$. To see this, suppose that $h(r) = 2x_1$ for some $r \in (u(b), u(x_1))$. Then h achieves a positive local minimum at some point $r_0 \in (u(b), u(x_1))$. At r_0 we have $h(r_0) > 0$, $h'(r_0) = 0$, and $h''(r_0) \geq 0$, so that

$$0 \leq \frac{h''(r_0)}{1 + (f'(r_0))^2} = \left(\frac{r}{2} - \frac{n-1}{r}\right) 2f'(r_0) - \frac{h(r_0)}{2} < 0,$$

which is a contradiction. Therefore, $h(r) < 2x_1$ for $r \in (u(b), u(x_1))$. Finally, to see $\delta(s) < 0$ when $s > 0$, we suppose to the contrary that $\delta(s) = 0$ for some $s > 0$. Set $r = u(x_1 + s) = u(x_1 - s)$. Then

$$2x_1 > h(r) = (x_1 + s) + (x_1 - s) = 2x_1,$$

which is a contradiction. We conclude that $\delta(s) < 0$ when $s > 0$. □

Now, we are ready to prove Proposition 7.

Proof of Proposition 7. We consider the case where the right end point of $\Lambda_k(\gamma[t])$ is the right end point of $\Lambda_{k+1}(\gamma[t])$. The case where the left end point of $\Lambda_k(\gamma[t])$ is the left end point of $\Lambda_{k+1}(\gamma[t])$ is similar.

Let $\Lambda_k(\gamma[t])$ be the graph of u_t, and let $\Lambda_{k+1}(\gamma[t])$, be the graph of v_t. Also, let the half-entire graph Λ_∞ be the graph of u_∞. With this notation, the solutions u_t converge to the half-entire graph u_∞. To prove the proposition, we need to show that the initial conditions $(v_t(0), v_t'(0))$ converge to $(u_\infty(0), u_\infty'(0))$ as $t \to t_\infty$. It is sufficient to show that for every sequence $t_i \to t_\infty$ there is a subsequence of $(v_i(0), v_i'(0))$ converging to $(u_\infty(0), u_\infty'(0))$. (Note that we are using the subscript notation i in place of t_i.)

First, we will show that every subsequence of $(v_i(0), v_i'(0))$ has a convergent subsequence. By choosing u_i sufficiently close to u_∞, we may assume that the

right end point of the graph of u_i is bounded away from the r-axis. Since the right end point of u_i is the same as the right end point of v_i, applying Lemma 12 and Lemma 13, we see that there are positive constants m, M, and L so that $m \leq v_i(0) \leq M$ and $v_i'(0) \geq -L$. We want to find an upper bound for $v_i'(0)$. Fix small $\varepsilon > 0$, and choose $C > 4\pi/\varepsilon$ so that $u_\infty < C$ on $[0, 2\varepsilon]$. By continuity we also assume that $u_i < C$ on $[0, 2\varepsilon]$. If $v_i'(0)$ is sufficiently large, then $v_i(x_0) = 2C$ for some $x_0 < \varepsilon$. We claim that v_i has a local maximum at some point in $(0, 2\varepsilon)$. Suppose to the contrary that v_i has no local maximum in $(0, 2\varepsilon)$. Then the rectangle R: $x_0 \leq x \leq x_0 + \varepsilon$, $C \leq r \leq 2C$ is contained in a simple region bounded by the image of the geodesic γ_i and the r-axis. Applying the Gauss-Bonnet formula we arrive at a contradiction, which proves the claim. It follows from Lemma 14 that the right end point of v_i is less than 4ε. Since the right end point of u_i is bounded away from the r-axis, we conclude that $v_i'(0)$ has an upper bound.

Now, let v_∞ be the solution of (4) corresponding to such a convergent subsequence. Notice that v_∞ is a half-entire graph in the first quadrant (otherwise, v_∞ has a right end point in the upper half-plane, and by continuity u_i cannot converge to u_∞). Next, we will show $v_\infty = u_\infty$.

Case 1. u_∞ and v_∞ are both quarter-spheres. Let p and q denote the right end points of u_∞ and v_∞, respectively. If $v_\infty \neq u_\infty$, then $q \neq p$, and there exists $\delta > 0$ so that $|p - q| > 2\delta$. For small $\varepsilon > 0$, depending on u_∞ and v_∞, we claim there exists a rectangle R of the form: $x_0 \leq x \leq x_0 + \delta$, $\varepsilon/2 \leq r \leq \varepsilon$ so that, for large i, the rectangle R is contained in a simple, compact region bounded by γ_i and possibly the r-axis. Notice that such a rectangle can be found in the region bounded by the two quarter-spheres, the x-axis, and possibly the r-axis. To establish the claim, we first consider the configuration where the x-coordinate of p is less than the x-coordinate of q. Then, a consideration of the convex shape of u_∞ near the point p shows that the solution u_i has an inflection point, for large i. Otherwise, the graph of u_i would not meet the graph of v_i. In fact, this inflection point must be close to p for large i. Following along u_i after this inflection point, we see that u_i is concave up and decreasing, and therefore it eventually reaches a local minimum. Applying Proposition 4 shows that u_i is concave up after this local minimum and consequently the graph of u_i is type $(j_0, +)$ for some j_0. It immediately follows that the graph of v_i is type $(j_1, -)$, for some j_1. Similar reasoning shows that the right end point of v_i is close to q, for large i. Therefore, for large i, the geodesic γ_i follows along the graph of u_∞ (getting close to p), then follows along to the x-axis (getting close to q), and finally travels back toward the r-axis along the graph of v_∞. The convexity of u_i after the inflection point near p shows that the rectangle R is contained in this region bounded by γ_i and possibly the r-axis, which proves the claim. When the x-coordinate of p is greater than the x-coordinate of q the proof of the claim is similar with the roles of u_i and v_i switched. To finish the proof of the lemma in Case 1, we observe that $\int_R r^{-2} dx dr = \delta/\varepsilon$, and an application of the Gauss-Bonnet formula (8) shows that this is impossible when ε is small. Hence $v_\infty = u_\infty$.

Case 2. u_∞ and v_∞ are both trumpets. Then there exist rays $r_\sigma(x) = \sigma x$ and $r_\tau(x) = \tau x$ so that u_∞ and v_∞ are asymptotic to r_σ and r_τ, respectively. If $u_\infty \neq v_\infty$, then $\sigma \neq \tau$. Now, the wedge between r_σ and r_τ has infinite area, and the same is true for the area of the wedge outside any compact set. Arguing as in the first case and using the property that the trumpets are asymptotic to the rays,

we can show there is a simple region bounded by the image of γ_i and the r-axis that encloses arbitrarily large area as $i \to \infty$. An application of the Gauss-Bonnet formula shows that this is impossible. The proof is similar when one of the trumpets is the cylinder.

Case 3. u_∞ is a quarter-sphere and v_∞ is a trumpet or a cylinder. It follows from Proposition 4 that $\Lambda_0(\gamma_i)$ is type $(i_0, +)$ for some i_0. Then, arguing as in the previous cases, we can show there is a simple region bounded by the image of γ_i and the r-axis that encloses arbitrarily large area as $i \to \infty$, and an application of the Gauss-Bonnet formula shows that this is impossible. □

Proof of Corollary 1. By continuity of solutions to (3), it suffices to consider the possible ways each type of graphical geodesic segment can converge to a half-entire graph.

We begin by considering the half-entire graphs in $\underline{T}$. Let $T = \Lambda_0(\gamma[0, r_T, \alpha_T])$ be a trumpet. Since the set of initial data (r, α) corresponding to half-entire graphs is one-dimensional, we can perturb the initial data to obtain solutions

$$\gamma_\epsilon := \gamma[0, r_T + \epsilon_r, \alpha_T + \epsilon_\alpha]$$

so that $\Lambda_0(\gamma_\epsilon)$ is not in $\underline{H}$ for arbitrarily small ϵ. Let $u_{k,\epsilon} : (a_{k,\epsilon}, b_{k,\epsilon}) \to (0, \infty)$ be the function whose graph is $\Lambda_k(\gamma_\epsilon)$. If $T \in \underline{T}^+$, then $a_{k,\epsilon}$ is bounded for small ϵ, so that $\lim_{x \to a_i} u'_{k,\epsilon}(x) = -\infty$. By construction, we have $b_{0,0} = \infty$ and $b_{0,\epsilon} < \infty$, for $\epsilon \neq 0$. There are two cases to consider: (a) $\lim_{x \to b_{0,\epsilon}} u'_{0,\epsilon}(x) = \infty$ and (b) $\lim_{x \to b_{0,\epsilon}} u'_{0,\epsilon}(x) = -\infty$.

In case (a), we claim that $u_{0,\epsilon}(x)$ is a globally convex function. If not, then the graph of $u_{0,\epsilon}(x)$ is type $(2, +)$. Since $u'_{0,\epsilon}(0) > 0$, we know that $u_{0,\epsilon}$ is convex in the second quadrant. It follows that there are points $0 < x_0 < x_1$ so that $u_{0,\epsilon}$ has a maximum at x_0 and a minimum at x_1. Since $u_{0,\epsilon}$ converges to a globally convex function, we have $x_0 \to \infty$ as $\epsilon \to 0$. We note that $u_{0,\epsilon}(x_1) < \sqrt{2(n-1)}$ so that $u_{0,\epsilon}$ intersects the cylinder between x_0 and x_1. Applying the Gauss-Bonnet formula to the region contained below the graph of $u_{0,\epsilon}$ and above the cylinder, we arrive at a contradiction (since the area of this region approaches ∞ as $\epsilon \to 0$). We conclude that $u_{0,\epsilon}$ is globally convex (and $T \notin \underline{\Lambda}(0, +)$). Applying Proposition 7 to γ_ϵ we see that $u_{1,\epsilon}(x) \to u_{0,0}(x)$ as $\epsilon \to 0$, and examining the possible types of curves, we see that the graph of $u_{1,\epsilon}$ must be type $(1, -)$ for small ϵ. This says that T is the limit of type $(0, +)$ and type $(1, -)$ graphical geodesic segments. In case (b), we similarly conclude that the graph of $u_{0,\epsilon}$ is type $(1, -)$ and the graph of $u_{1,\epsilon}$ is type $(0, +)$ for small ϵ. In both cases we get that T is the limit of type $(0, +)$ and type $(1, -)$ graphical geodesic segments.

Next, we consider the half-entire graphs in $\underline{I}$. Let I be an inner quarter-sphere (or the sphere). By performing a similar perturbation as above, we obtain curves γ_ϵ with $\Lambda_0(\gamma_\epsilon) \notin \underline{H}$ converging to I as $\epsilon \to 0$. If $I \in \underline{I}^+$, then it is type $(0, -)$, and an argument similar to the one in the trumpet case shows that $\Lambda_0(\gamma_\epsilon)$ and $\Lambda_1(\gamma_\epsilon)$ are type $(0, -)$ and type $(1, +)$ (or type $(1, +)$ and type $(0, -)$). It follows that I is the limit of type $(0, -)$ and type $(1, +)$ graphical geodesic segments. A similar result holds for $\underline{I}^-$. Also, since the sphere $\mathcal{S}$ is the limit of elements in $\underline{I}^+$ (and $\underline{I}^-$), we see that $\mathcal{S}$ is the limit of type $(0, -)$, type $(1, -)$, and type $(1, +)$ graphical geodesic segments.

Lastly, we consider the outer quarter-spheres. Arguing as we did for the inner quarter-spheres, we have that $O \in \underline{O}^+$ is the limit of type $(1, -)$ and type $(2, +)$

graphical geodesic segments. A similar result holds for $\underline{O}^-$. We note that $\mathcal{S}$ is also the limit of type $(2,+)$ graphical geodesic segments.

Finally, by considering the possible limiting shapes of different types of curves and using the continuity of solutions to (3), we can complete the proof of the corollary. For instance, the limit of type $(1,+)$ curves can only be type $(0,+)$, type $(0,-)$, or type $(1,+)$, and by continuity such a limit cannot be in $\underline{T}^+$, $\underline{I}^-$ or $\underline{O}^+$. □

6. Behavior near known solutions

In Section 5, we showed that whenever a continuous family of maximally extended graphical geodesic segments in $\underline{\Lambda}$ changes types, it must do so through a half-entire graph (see Corollary 1). In this way, we can construct complete self-shrinkers by finding a family of solutions $\gamma[t]$ to a continuous shooting problem whose ordered decompositions into graphical geodesic segments $\Lambda_k(\gamma[t])$ have different types for some $k \geq 0$. In order to carry out this procedure, we first establish the asymptotic behavior of solutions near the plane, the cylinder, and Angenent's torus.

6.1. **Behavior near the plane.** To begin, we consider the continuous family of solutions $Q[t]$ to (3) introduced in Section 3.1. Recall that $\Lambda_0(Q[t])$ is a quarter-sphere (when $t \neq 0$). By Proposition 6, we know the types of the maximally extended graphical geodesic segments $\Lambda_0(Q[t])$, and we are interested in describing the types of $\Lambda_k(Q[t])$ when $t > 0$ is small. The following two lemmas are consequences of several results from Section 3.2.

Lemma 15. *Let $\gamma = \gamma[0, r_0, \alpha_0]$ be a solution to the shooting problem (9), (10), and let $\Lambda_0(\gamma)$ be the graph of $u : (a,b) \to (0,\infty)$. If $u(0) \in (m_1, \sqrt{2(n-1)})$ and $u'(0) < 0$ (so that $r_0 \in (m_1, \sqrt{2(n-1)})$ and $\alpha_0 \in (-\pi/2, 0)$), then $\Lambda_1(\gamma)$ exists, and it can be written as the graph of $v : (c,b) \to (0,\infty)$. If $u'(0)$ is sufficiently negative, then $\Lambda_1(\gamma)$ is type $(0,-)$ with $v(0) \in (\sqrt{2n}, M_1)$ and $v'(0) < 0$. Moreover, $v'(0) \to -\infty$ as $u'(0) \to -\infty$.*

Proof. Let $u : (a,b) \to (0,\infty)$ denote the maximally extended solution to (4) whose graph is the graphical geodesic segment $\Lambda_0(\gamma)$. By assumption $u(0) < \sqrt{2(n-1)}$ and $u'(0) < 0$, and it follows from the work in Section 3.2 that $b < \infty$ and $0 < u(b) < \infty$, and $u'' > 0$ on $[0,b)$ (see Lemma 8 and Lemma 9). Since b and $u(b)$ are finite, we conclude that $\Lambda_1(\gamma)$ exists.

When $u'(0) \to -\infty$, it follows from Lemma 13 that $b \to 0$. We note that $u(x)$ achieves its minimum over $[0,b)$ at an interior point. By the continuity of equation (6), this minimum value approaches 0 as $u'(0) \to -\infty$. Applying Lemma 3, we have $u(b) < \sqrt{2(n-1)}$.

Now, let f denote the solution to (6) with $f(u(b)) = b$ and $f'(u(b)) = 0$. Then f is concave down, and using the continuity of equation (6), we see that the domain of f approaches $(0,\infty)$ as $u'(0) \to -\infty$. Applying Lemma 2 we conclude that the graph of f crosses the r-axis below M_1, and the slope at this point approaches 0 as $u'(0) \to -\infty$. In addition, when b is small, the comparison arguments used in the proof of Lemma 18 in the Appendix show that the graph of f crosses the sphere at least once in the first quadrant. Also, when b is small, the slope of $f(r)$ may be chosen small for $r \in [u(b), \sqrt{2n}]$ (since the graph of f is close to the plane), and

we see that the graph of f crosses the sphere exactly once in the first quadrant. Therefore, $v(0) \in (\sqrt{2n}, M_1)$ and $v'(0) \to -\infty$ as $u'(0) \to -\infty$.

Finally, we claim that v has a maximum in the second quadrant and $v'' < 0$ when b is small. To see this, we first note that the graph of v intersects the r-axis above the cylinder with negative slope when b is small. Therefore, v is not a trumpet and it has a maximum in the second quadrant. Now, this maximum value goes to ∞ as b goes to 0, and arguing as in Part 1 in the proof of Lemma 14 and also using the convexity of f from the previous paragraph, we conclude that $v'' < 0$ for sufficiently small b. Therefore, $\Lambda_1(\gamma)$ is type $(0, -)$ when $u'(0)$ is sufficiently negative. □

Lemma 16. *Let $\gamma = \gamma[0, r_0, \alpha_0]$ be a solution to the shooting problem (9), (10), and let $\Lambda_0(\gamma)$ be the graph of $u : (a, b) \to (0, \infty)$. If $u(0) \in (\sqrt{2n}, M_1)$ and $u'(0) > 0$ (so that $r_0 \in (\sqrt{2n}, M_1)$ and $\alpha_0 \in (0, \pi/2)$), then $\Lambda_1(\gamma)$ exists, and it can be written as the graph of $v : (c, b) \to (0, \infty)$. If $u'(0)$ is sufficiently large, then $\Lambda_1(\gamma)$ is type $(0, +)$ with $v(0) \in (m_1, \sqrt{2(n-1)})$ and $v'(0) > 0$. Moreover, $v'(0) \to \infty$ as $u'(0) \to \infty$.*

Proof. Let $u : (a, b) \to (0, \infty)$ denote the maximally extended solution to (4) whose graph is the graphical geodesic segment $\Lambda_0(\gamma)$. By assumption $u(0) > \sqrt{2n}$ and $u'(0) > 0$, it follows from the work in Section 3.2 that $b < \infty$, $0 < u(b) < \infty$ (see Lemma 8). Since b and $u(b)$ are finite, we conclude that $\Lambda_1(\gamma)$ exists. In addition, we note that u achieves a local maximum at some point $x_1 > 0$.

When $u'(0) \to \infty$, it follows from the continuity of equation (6), that $u(x_1) \to \infty$. Using Part 1 in the proof of Lemma 14, we have $\Lambda_1(\gamma)$ is type $(0, +)$ and $u(b) > u(x_1) - 2$ for $u'(0)$ sufficiently large. The triangle with vertices $(0, \sqrt{2(n-1)})$, $(0, \sqrt{2n})$, and $(x_1, u(x_1))$ is contained in a simple region bounded by the image of γ and the r-axis, and it follows from the Gauss-Bonnet formula (8) that $x_1 \to 0$ as $u(x_1) \to \infty$. Applying Lemma 14, we see that $b \to 0$ as $u'(0) \to \infty$.

Now, let f denote the solution to (6) with $f(u(b)) = b$ and $f'(u(b)) = 0$. By choosing b sufficiently small, we may assume that $u(b) > \sqrt{2n}$. Then f is concave down and $f'(\sqrt{2n}) > 0$. Using equation (6) we have $f'(\sqrt{2n}) < \sqrt{n/2} f(\sqrt{2n})$. Then using $f(\sqrt{2n}) < b$ and the continuity of equation (6), at the point $r = \sqrt{2n}$, we see that the domain of f approaches $(0, \infty)$ as $u'(0) \to \infty$. Applying Lemma 3 we conclude that f crosses the r-axis above m_1, and the slope at this point approaches 0 as $u'(0) \to \infty$. Therefore, $v(0) \in (m_1, \sqrt{2n})$, and $v'(0) \to \infty$ as $u'(0) \to \infty$. □

Now, we can describe the asymptotic behavior of the solutions $Q[t]$ near the plane.

Proposition 8. *For each $N > 0$, there exists $\varepsilon > 0$ so that whenever $0 < t < \varepsilon$, the graphical geodesic segment $\Lambda_k(Q[t])$ exists for $0 \le k \le N$. Moreover, $\Lambda_k(Q[t])$ is type $(0, -)$ when k is even, and $\Lambda_k(Q[t])$ is type $(0, +)$ when k is odd.*

Proof. We know that $\Lambda_0(Q[t])$ is type $(0, -)$ when $t < \sqrt{2n}$. Let $u : (a, t) \to (0, \infty)$ denote the maximally extended solution to (4) whose graph is the graphical geodesic segment $\Lambda_0(Q[t])$. By Proposition 1, $u(0) \in (\sqrt{2n}, M_1)$ and $u'(0) < 0$. By continuity, we have $u'(0) \to -\infty$ as $t \to 0$. The proposition now follows from repeated applications of Lemma 16 and Lemma 15. (Here Lemma 16 is applied to the reflection of the solution across the r-axis.) □

6.2. **Behavior near the cylinder.** Next, we study the continuous family of solutions $\gamma_t = \gamma[0,t,0]$ to the shooting problem (9), (10). By Lemma 5 we know that $\Lambda_0(\gamma_t)$ is type $(0,+)$ when $t < \sqrt{2(n-1)}$. The following lemma about solutions near the cylinder will be used to describe the shape of γ_t when t is close to $\sqrt{2(n-1)}$.

Lemma 17. *Let $\gamma = \gamma[0,r_0,\alpha_0]$ be a solution to the shooting problem (9), (10), and let $\Lambda_0(\gamma)$ be the graph of $u : (a,b) \to (0,\infty)$. If $u(0) < \sqrt{2n}$ and $u'(0) < 0$ (so that $r_0 < \sqrt{2n}$ and $\alpha_0 \in (-\pi/2, 0)$), then $\Lambda_1(\gamma)$ exists, and it can be written as the graph of $v : (c,b) \to (0,\infty)$. If $u(0)$ is sufficiently close to $\sqrt{2(n-1)}$ and $u'(0)$ is sufficiently close to 0, then $\Lambda_1(\gamma)$ is type $(1,-)$ with $v'(0) > 0$. Moreover, $v(0) \to \sqrt{2(n-1)}$ and $v'(0) \to 0$ as $u(0) \to \sqrt{2(n-1)}$ and $u'(0) \to 0$.*

Proof. By the work in Section 3.2, we know that $\Lambda_0(\gamma)$ is type $(i_0,+)$ and it has a finite right end point. Therefore, $\Lambda_1(\gamma)$ exists and has type $(i_1,-)$. Applying Proposition 7, we see that $\Lambda_1(\gamma)$ converges to the cylinder as $u(0) \to \sqrt{2(n-1)}$ and $u'(0) \to 0$. In particular, $v(0) \to \sqrt{2(n-1)}$ and $v'(0) \to 0$. Using Lemma 10 and the continuity of solutions to (3), we observe that a maximally extended graphical geodesic segment, which intersects the r-axis perpendicularly between the sphere and the cylinder, is type $(2,+)$. Combining this observation with the work in Section 3.2 shows that $v'(0) > 0$, and consequently $\Lambda_1(\gamma)$ is type $(1,-)$. □

Now, we can describe the asymptotic behavior of the geodesics $\gamma[0,t,0]$ near the cylinder.

Proposition 9. *Let $\gamma_t = \gamma[0,t,0]$. For each $N > 0$, there exists $\varepsilon > 0$ so that whenever $\sqrt{2(n-1)} - \varepsilon < t < \sqrt{2(n-1)}$, the graphical geodesic segment $\Lambda_k(\gamma_t)$ exists for $0 \le k \le N$. Moreover, $\Lambda_k(\gamma_t)$ is type $(1,-)$ when k is odd, and $\Lambda_k(\gamma_t)$ is type $(1,+)$ when $k \ge 2$ is even.*

Proof. By Lemma 5, $\Lambda_0(\gamma_t)$ is type $(0,+)$, and we know that $\Lambda_1(\gamma)$ exists. Let $\Lambda_1(\gamma)$ be the graph of $v : (c,b) \to (0,\infty)$. Arguing as in the proof of Lemma 17, we see that $\Lambda_1(\gamma_t)$ is type $(1,-)$ and $v'(0) > 0$ for t sufficiently close to $\sqrt{2(n-1)}$. Moreover, $\Lambda_1(\gamma_t)$ converges to the cylinder as $t \to \sqrt{2(n-1)}$. The proposition follows from repeated applications of Lemma 17. (Note that when k is even we apply Lemma 17 to the reflection of the solution across the r-axis.) □

6.3. **Behavior near Angenent's torus.** We continue the study of the solutions $\gamma_t = \gamma[0,t,0]$ to the shooting problem (9), (10) by illustrating two procedures for constructing self-shrinkers. We prove the result due to Angenent [3] that there is an embedded torus self-shrinker, and we also prove the result from [10] that there is an immersed sphere self-shrinker.

Consider $\gamma_t = \gamma[0,t,0]$, where $t < \sqrt{2(n-1)}$. From Lemma 5 we know that $\Lambda_0(\gamma_t)$ is type $(0,+)$, and from the work in Section 3.2, we know that $\Lambda_1(\gamma_t)$ exists. Proposition 9 tells us that $\Lambda_1(\gamma_t)$ is type $(1,-)$ when t is close to $\sqrt{2(n-1)}$. Moreover, $\Lambda_1(\gamma_t)$ has a local maximum in the first quadrant. When t is close to 0, it follows from the proof of Lemma 15 that $\Lambda_1(\gamma_t)$ is type $(0,-)$ with a local maximum in the second quadrant.

There are two notable differences in the graphical geodesic segments $\Lambda_1(\gamma_t)$ when t is close to $\sqrt{2(n-1)}$ and when t is close to 0. One difference is the location of the local maximum, and the other difference is the curve type. As t decreases from

$\sqrt{2(n-1)}$ to 0, there is a first initial height $t = r_{Ang}$ for which the local maximum of $\Lambda_1(\gamma_t)$ intersects the r-axis. (More rigorously, let r_{Ang} denote the infimum of the set of $r < \sqrt{2(n-1)}$ with the property that for $t > r$, the maximum of $\Lambda_1(\gamma_t)$ occurs in the first quadrant.) Notice that $r_{Ang} > 0$, and by the symmetry of (3) with respect to reflections across the r-axis, the image of $\gamma_{r_{Ang}}$ is a closed geodesic. Moreover, $\gamma_{r_{Ang}}$ is convex, and it is also the profile curve for an embedded torus self-shrinker. We will refer to the image of $\gamma_{r_{Ang}}$ as Angenent's torus.

Since $\Lambda_1(\gamma_{r_{Ang}})$ is type $(0,-)$, the graphical geodesic segments $\Lambda_1(\gamma_t)$ change type as t decreases from $\sqrt{2(n-1)}$ to r_{Ang}. By continuity, the right end points of $\Lambda_1(\gamma_t)$ remain bounded away from the r-axis in a compact subset of $\mathbb{H}$ when t is between, say, $\sqrt{2(n-1)}-\varepsilon$ and r_{Ang}, and applying Corollary 1 we see that there is $r_1 > r_{Ang}$ so that $\Lambda_1(\gamma_{r_1}) \in \underline{I}^-$. Therefore, using the symmetry of (3) with respect to reflections across the r-axis, we see that γ_{r_1} is the profile curve for an immersed sphere self-shrinker.

We end this section with a description of the asymptotic behavior of solutions to (3) near Angenet's torus $\gamma_{r_{Ang}}$.

Proposition 10. *Let $\gamma_t = \gamma[0,t,0]$. For each $N > 0$, there exists $\varepsilon > 0$ so that whenever $r_{Ang} < t < r_{Ang} + \varepsilon$, the maximally extended graphical geodesic segment $\Lambda_k(\gamma_t)$ exists for $0 \leq k \leq N$. Moreover, $\Lambda_k(\gamma_t)$ is type $(0,+)$ when k is even and $\Lambda_k(\gamma_t)$ is type $(0,-)$ when k is odd.*

Proof. The proposition follows from the continuity of geodesics and the convexity of $\gamma_{r_{Ang}}$. □

7. Construction of self-shrinkers

In this section we construct an infinite number of sphere and plane self-shrinkers near the plane in Theorem 3, an infinite number of sphere and torus self-shrinkers near the cylinder in Theorem 4, and an infinite number of sphere and cylinder self-shrinkers near Angenent's torus in Theorem 5. It follows from the asymptotic behavior of the trumpets at infinity [22, Theorem 3] that the plane and cylinder self-shrinkers we construct are complete and have polynomial volume growth. In particular, by Colding and Minicozzi's theorem for complete self-shrinkers with polynomial volume growth in [7], the self-shrinkers we construct in this section are not F-stable.

Theorem 3. *There is a decreasing sequence of positive numbers $t_0 > t_1 > \cdots$ so that $Q[t_k]$ is the profile curve for an S^n self-shrinker when k is even and a complete $\mathbb{R}^n$ self-shrinker when k is odd. Moreover, the image of $Q[t_k]$ is the union of $(k+1)$ maximally extended graphical geodesic segments.*

Proof. The proof is by induction. For the base case, we define $t_0 = \sqrt{2n}$ so that $Q[t_0]$ is the profile curve for the round sphere self-shrinker. We note that $\Lambda_0(Q[t])$ is type $(0,-)$ for $0 < t < t_0$ (this follows from Proposition 6). We also note that $\Lambda_1(Q[t])$ exists for $0 < t < t_0$, since $Q[\sqrt{2n}]$ is the only profile curve corresponding to an embedded S^n self-shrinker with rotational symmetry.

Continuing the base case, we note that for fixed $\varepsilon > 0$ the left end point of $\Lambda_1(Q[t])$ is bounded away from the x-axis inside a compact subset of $\mathbb{H}$ when $\varepsilon \leq t \leq t_0 - \varepsilon$. When t is close to and greater than 0, it follows from Proposition 8 that $\Lambda_1(Q[t])$ is type $(0,+)$. Applying Proposition 7 to the left end point of $\Lambda_0(Q[t_0])$

shows that $\Lambda_1(Q[t])$ is either type $(1,-)$ or type $(2,+)$ when t is close to and less than $t_0 = \sqrt{2n}$. In particular, by choosing ε small enough, we see that the graphical geodesic segments $\Lambda_1(Q[t])$ change type as t increases from ε to $t_0 - \varepsilon$. It follows that the right end point $\Lambda_1(Q[t])$ is a half-entire graph for some t between ε and $t_0 - \varepsilon$. We define t_1 to be the first $t > 0$ such that $\Lambda_1(Q[t])$ is a half-entire graph. Then $0 < t_1 < t_0$, and by Corollary 1 the graphical geodesic segment $\Lambda_1(Q[t_1])$ is a trumpet in the first quadrant.

For the inductive case, we assume that the positive numbers $t_0 > t_1 > \cdots > t_N$ are defined: t_k is the first $t > 0$ such that $\Lambda_k(Q[t])$ is a half-entire graph. We also assume that $\Lambda_i(Q[t_k])$ is type $(0,-)$ when $i \leq k$ is even, and it is type $(0,+)$ when $i \leq k$ is odd. In addition, we assume that $\Lambda_k(Q[t_k])$ is an inner quarter-sphere in the second quadrant when k is even, and it is a trumpet in the first quadrant when k is odd. We will show there exists a positive number $t_{N+1} < t_N$ such that t_{N+1} is the first $t > 0$ for which $\Lambda_{N+1}(Q[t])$ is a half-entire graph. When N is odd, we will show that $\Lambda_{N+1}(Q[t_{N+1}])$ is an inner quarter-sphere in the second quadrant, and when N is even, we will show that $\Lambda_{N+1}(Q[t_{N+1}])$ is a trumpet in the first quadrant.

Suppose N is odd. Then $\Lambda_{N+1}(Q[t])$ exists, for $0 < t < t_N$. We note that for fixed $\varepsilon > 0$ the right end point of $\Lambda_{N+1}(Q[t])$ remains bounded away from the x-axis in a compact subset of $\mathbb{H}$ when $\varepsilon \leq t \leq t_N - \varepsilon$. When t is close to and greater than 0 it follows from Proposition 8 that $\Lambda_{N+1}(Q[t])$ is type $(0,-)$. Applying Proposition 7 shows that $\Lambda_{N+1}(Q[t])$ is type $(1,-)$ when t is close to and less than t_N. In particular, by choosing ε small enough, we may assume that the graphical geodesic segments $\Lambda_{N+1}(Q[t])$ change type as t increases from ε to $t_N - \varepsilon$. It follows that $\Lambda_{N+1}(Q[t])$ is a half-entire graph for some t between ε and $t_N - \varepsilon$. We define t_{N+1} to be the first $t > 0$ such that $\Lambda_{N+1}(Q[t])$ is a half-entire graph. Then $t_{N+1} < t_N$, and by Corollary 1 the graphical geodesic segment $\Lambda_{N+1}(Q[t_{N+1}])$ is an inner quarter-sphere in the second quadrant.

Suppose N is even. Then $\Lambda_{N+1}(Q[t])$ exists, for $0 < t < t_N$. We note that for fixed $\varepsilon > 0$ the left end point of $\Lambda_{N+1}(Q[t])$ remains bounded away from the x-axis in a compact subset of $\mathbb{H}$ when $\varepsilon \leq t \leq t_N - \varepsilon$. When t is close to and greater than 0 it follows from Proposition 8 that $\Lambda_{N+1}(Q[t])$ is type $(0,+)$. Applying Proposition 7 shows that $\Lambda_{N+1}(Q[t])$ is type $(1,-)$ when t is close to and less than t_N. In particular, by choosing ε small enough, we may assume that the graphical geodesic segments $\Lambda_{N+1}(Q[t])$ change type as t increases from ε to $t_N - \varepsilon$. It follows that $\Lambda_{N+1}(Q[t])$ is a half-entire graph for some t between ε and $t_N - \varepsilon$. We define t_{N+1} to be the first $t > 0$ such that $\Lambda_{N+1}(Q[t])$ is a half-entire graph. Then $t_{N+1} < t_N$, and by Corollary 1 the graphical geodesic segment $\Lambda_{N+1}(Q[t_{N+1}])$ is a trumpet in the first quadrant. This completes the proof of the inductive case. □

Theorem 4. *There is an increasing sequence of positive numbers $t_0 < t_1 < \cdots < \sqrt{2(n-1)}$ so that $\gamma[0, t_k, 0]$ is the profile curve for an $S^1 \times S^{n-1}$ self-shrinker when k is even and an S^n self-shrinker when k is odd. Moreover, the image of $\gamma[0, t_k, 0]$ is the union of $(k+2)$ distinct maximally extended graphical geodesic segments.*

Proof. The proof is by induction; it is similar to the proof of Theorem 3. Let $\gamma_t = \gamma[0, t, 0]$. Since we are shooting perpendicularly to the r-axis, it follows from the symmetry of (3) with respect to reflections about the r-axis that γ_t has a reflection symmetry about the r-axis. In order to construct the profile curve of a

complete self-shrinker, it suffices to find k and t so that either $\Lambda_k(\gamma_t)$ is a half-entire graph or it intersects the r-axis perpendicularly.

By Lemma 5, we know that $\Lambda_0(\gamma_t)$ is type $(0,+)$ when $t < \sqrt{2(n-1)}$. It follows from Proposition 9 that for each $N > 0$, there exists $\varepsilon > 0$ so that whenever $\sqrt{2(n-1)} - \varepsilon < t < \sqrt{2(n-1)}$, the graphical geodesic segment $\Lambda_k(\gamma_t)$ exists for $0 \leq k \leq N$. Moreover, $\Lambda_k(\gamma_t)$ is type $(1,-)$ when k is odd, and $\Lambda_k(\gamma_t)$ is type $(1,+)$ when $k \geq 2$ is even.

For the base case, we define t_0 to be the largest $t < \sqrt{2(n-1)}$ such that $\Lambda_1(\gamma_t)$ intersects the r-axis perpendicularly. Then $t_0 = r_{Ang}$ and the image of γ_{t_1} is the closed embedded convex curve constructed in Section 6.3.

Continuing the base case, since $\Lambda_1(\gamma_t)$ is type $(1,-)$ when t is close to $\sqrt{2(n-1)}$ and type $(0,-)$ when t is close to t_0, there is some t between $\sqrt{2(n-1)}$ and t_0 such that $\Lambda_1(\gamma_t)$ is a half-entire graph. We define t_1 to be the largest $t < \sqrt{2(n-1)}$ such that $\Lambda_1(\gamma_t)$ is a half-entire graph. By Corollary 1, the half-entire graph $\Lambda_1(\gamma_{t_1})$ is an inner quarter-sphere in the second quadrant. Notice that $\Lambda_0(\gamma_{t_1})$ is type $(0,+)$, $\Lambda_1(\gamma_{t_1}) \in \underline{I}^-$, and $\Lambda_{-1}(\gamma_{t_1}) \in \underline{I}^+$ so that γ_{t_1} is the union of 3 maximally extended graphical geodesic segments.

For the inductive case, we assume that $t_1 < t_3 < \cdots < t_{2N-1}$ are defined: t_{2k-1} is the largest $t < \sqrt{2(n-1)}$ such that $\Lambda_k(\gamma_t)$ is a half-entire graph. We also assume that $\Lambda_N(\gamma_{t_{2N-1}})$ is an inner quarter-sphere. Suppose $\Lambda_N(\gamma_{t_{2N-1}})$ is an inner quarter-sphere in the first quadrant. By Proposition 7 we have $\Lambda_{N+1}(\gamma_t)$ is type $(0,-)$ with a local maximum in the second quadrant when $t > t_{2N-1}$ is close to t_{2N-1}. It follows that the type of $\Lambda_{N+1}(\gamma_t)$ changes as t decreases from $\sqrt{2(n-1)}$ to t_{2N-1}, so we can define $t_{2N+1} > t_{2N-1}$ to be the largest $t < \sqrt{2(n-1)}$ such that $\Lambda_{N+1}(\gamma_t)$ is a half-entire graph. Then $\Lambda_{N+1}(\gamma_{t_{2N+1}})$ is an inner quarter-sphere in the second quadrant (since it is the limit of type $(1,-)$ graphical geodesic segments). Therefore, the solution $\gamma_{t_{2N+1}}$ is the union of $(2N+3)$ maximally extended graphical geodesic segments, and its rotation about the x-axis is an immersed S^n self-shrinker. Furthermore, since the local maximums of $\Lambda_{N+1}(\gamma_{t_{2N+1}})$ and $\Lambda_{N+1}(\gamma_t)$ for t near t_{2N-1} are in different quadrants, there exists t_{2N} between t_{2N-1} and t_{2N+1} so that $\Lambda_{N+1}(\gamma_{t_{2N}})$ intersects the r-axis perpendicularly. Then $\gamma_{t_{2N}}$ is the union of $(2N+2)$ maximally extended graphical geodesic segments, and its rotation about the x-axis is an immersed $S^1 \times S^{n-1}$ self-shrinker. This completes the proof of the inductive case. □

Theorem 5. *There is a decreasing sequence of positive numbers $t_0 > t_1 > \cdots > r_{Ang}$ so that $\gamma[0,t_k,0]$ is the profile curve for a complete $\mathbb{R}^1 \times S^{n-1}$ self-shrinker when k is even and an S^n self-shrinker when k is odd. Moreover, the image of $\gamma[0,t_k,0]$ is the union of $(2k+1)$ maximally extended graphical geodesic segments.*

Proof. The proof is by induction; it is similar to the proofs of Theorem 3 and Theorem 4, and we provide a sketch. Let $\gamma_t = \gamma[0,t,0]$. Given $N > 0$, there exists $\varepsilon > 0$ so that whenever $r_{Ang} < t < r_{Ang} + \varepsilon$, the graphical geodesic segment $\Lambda_k(\gamma_t)$ exists for $0 \leq k \leq N$. Moreover, $\Lambda_k(\gamma_t)$ is type $(0,+)$ when k is even, and it is type $(0,-)$ when k is odd. For the base case, we define $t_0 = \sqrt{2(n-1)}$, so that the image of γ_{t_0} is the cylinder $\mathcal{C}$. For the general case, we define t_k to be the first $t > r_{ang}$ such that $\Lambda_k(\gamma_t)$ is a half-entire graph. Then $\Lambda_k(\gamma_{t_k})$ is either a trumpet in the first quadrant or an inner quarter-sphere in the second quadrant, depending

on whether it is the limit of type $(0,+)$ graphical geodesic segments or type $(0,-)$ graphical geodesic segments, respectively. □

Appendix A: Comparison results for quarter-spheres

In this appendix we prove some comparison results for quarter-spheres. The main application of these results is that an inner quarter-sphere first intersects the r-axis outside of the sphere, and an outer quarter-sphere first intersects the r-axis inside the sphere.

Let f and g be solutions to

$$\frac{f''}{1+(f')^2} = \left(\frac{r}{2} - \frac{n-1}{r}\right) f' - \frac{1}{2} f. \tag{15}$$

We are interested in the shooting problem where $f'(0) = g'(0) = 0$ and $g(0) > f(0) > 0$.

In particular, we will consider the case where g is the sphere ($g(r) = \sqrt{2n - r^2}$) and f is an inner quarter-sphere. In this setting, we know that f is decreasing, concave down, and it crosses the r-axis before its slope blows-up (see [10, Corollary 3.3]). We want to show that f crosses the r-axis outside of the sphere.

We will use the following identities at 0 for solutions to (15):

$$f'(0) = 0, \quad f''(0) = -\frac{1}{2n} f(0), \quad f'''(0) = 0, \quad f^{(iv)}(0) = -\frac{3}{4n(n+2)} \left(\frac{f(0)^3}{n^2} + f(0)\right). \tag{16}$$

These identities follow from l'Hôpital's rule applied to (15) and its derivatives.

Lemma 18. *If f is a solution to* (15) *with $f(0) < \sqrt{2n}$, then f must intersect the sphere before it crosses the r-axis.*

Proof. Suppose f does not intersect g (the sphere) before it crosses the r-axis. Let $r_0 > 0$ be the point where f crosses the r-axis. Then $g > f$ on $[0, r_0)$.

We consider the function $v = \frac{f}{g}$, which satisfies

$$v' = \frac{f' - vg'}{g}$$

and

$$v'' = \frac{f'' - vg''}{g} - 2\frac{g'}{g} v'.$$

Now, using l'Hôpital's rule and the above identities at 0, we have $v'(0) = 0$ and $v''(0) = 0$. Similarly, $v'''(0) = 0$, and $v^{(iv)}(0) = -\frac{3}{4n^3(n+2)} v(0)[f(0)^2 - g(0)^2] > 0$, where we use the non-linear dependence of $f^{(iv)}(0)$ on $f(0)$ in the last equality. It follows that v is increasing near 0. Since $v(0) > 0$ and $\lim_{r \to r_0} v(r) = 0$ (where we use l'Hôpital's rule if $r_0 = \sqrt{2n}$), we see that v must achieve its supremum over $(0, r_0)$ at an interior point, say $\bar{r}$.

By assumption, $0 < v < 1$ in $(0, r_0)$, and in particular $0 < v(\bar{r}) < 1$. We compute $v''(\bar{r})$. Using $v'(\bar{r}) = 0$, we have at $\bar{r}$:

$$vg'' = (1 + (g')^2) \left[\left(\frac{r}{2} - \frac{n-1}{r}\right) f' - \frac{1}{2} f\right]$$

so that

$$f'' - vg'' = \left((f')^2 - (g')^2\right)\left[\left(\frac{r}{2} - \frac{n-1}{r}\right)f' - \frac{1}{2}f\right] = (v^2-1)(g')^2\frac{f''}{1+(f')^2}.$$

Therefore, at $\bar{r}$:

$$v'' = \frac{f'' - vg''}{g} = (v^2-1)\frac{(g')^2}{g}\frac{f''}{1+(f')^2} > 0,$$

which contradicts the fact that v has a maximum at $\bar{r}$. □

Lemma 19. *If f is a solution to (15) with $f(0) < \sqrt{2n}$, then f can only intersect the sphere once before it crosses the r-axis.*

Proof. Suppose f intersects g (the sphere) at two points before it crosses the r-axis: say r_1 and r_2, where $0 < r_1 < r_2$. Since $g(0) > f(0)$, we may assume that $f > g$ on (r_1, r_2). We may also assume that $r_2 < \sqrt{2n}$ (otherwise, f would intersect the r-axis perpendicularly at $\sqrt{2n}$, contradicting Huisken's theorem).

We consider the function $w = \frac{f'}{g'}$, which satisfies

$$w' = \frac{f'' - wg''}{g'}$$

and

$$w'' = \frac{f''' - wg'''}{g'} - 2\frac{g''}{g'}w'.$$

Now, using l'Hôpital's rule and the above identities at 0, we have $w(0) = \frac{f''(0)}{g''(0)} = \frac{f(0)}{g(0)} < 1$ and $w'(0) = 0$. Furthermore, using the non-linear dependence of $g^{(iv)}(0)$ on $g(0)$, we have $w''(0) = \frac{1}{2n^2(n+2)}w(0)[f(0)^2 - g(0)^2] < 0$. It follows that w is decreasing near 0. By assumption, we have $w(r_2) \geq 1$, and consequently, w must achieve its infimum on $(0, r_2)$ at an interior point, say $\bar{r}$.

Recall

$$f''' = \left(1+(f')^2\right)\left[\frac{2f'(f'')^2}{(1+(f')^2)^2} + \left(\frac{r}{2} - \frac{n-1}{r}\right)f'' + \frac{n-1}{r^2}f'\right].$$

Using $w'(\bar{r})$, we have at $\bar{r}$:

$$\begin{aligned}\frac{2f'(f'')^2}{1+(f')^2} - w\frac{2g'(g'')^2}{1+(g')^2} &= 2f'\left[\frac{(f'')^2}{1+(f')^2} - \frac{(g'')^2}{1+(g')^2}\right] \\ &= 2f'(g'')^2\left[\frac{w^2-1}{(1+(f')^2)(1+(g')^2)}\right].\end{aligned}$$

Also, at $\bar{r}$:

$$\left[\left(\frac{r}{2} - \frac{n-1}{r}\right)f'' + \frac{n-1}{r^2}f'\right] - w\left[\left(\frac{r}{2} - \frac{n-1}{r}\right)g'' + \frac{n-1}{r^2}g'\right] = 0$$

and

$$\begin{aligned}(f')^2\left[\left(\frac{r}{2} - \frac{n-1}{r}\right)f'' + \frac{n-1}{r^2}f'\right] - w\,(g')^2\left[\left(\frac{r}{2} - \frac{n-1}{r}\right)g'' + \frac{n-1}{r^2}g'\right] \\ = w\,(g')^2(w^2-1)\left[\left(\frac{r}{2} - \frac{n-1}{r}\right)g'' + \frac{n-1}{r^2}g'\right].\end{aligned}$$

Therefore, at $\bar{r}$:

$$\begin{aligned} w'' &= \frac{f''' - wg'''}{g'} \\ &= \left\{ \frac{2w(g'')^2}{(1+(f')^2)(1+(g')^2)} + wg' \left[\left(\frac{1}{2}r - \frac{n-1}{r} \right) g'' + \frac{n-1}{r^2} g' \right] \right\} (w^2-1) \\ &= \left\{ \frac{2w(g'')^2}{(1+(f')^2)(1+(g')^2)} - wg' \frac{r}{(2n-r^2)^{3/2}} \right\} (w^2-1), \end{aligned}$$

where we used $g(r) = \sqrt{2n-r^2}$ in the last equality. Since $w(\bar{r}) < w(0) < 1$, we have $w''(\bar{r}) < 0$, which contradicts the fact that w has a minimum at $\bar{r}$. □

We have the following consequence of Lemma 18 and Lemma 19.

Proposition 11. *An inner quarter-sphere intersects the sphere exactly once before it crosses the r-axis.*

When $f(0) > \sqrt{2n}$, similar arguments show that f blows-up at a point $r_* < \sqrt{2n}$. Assuming $f(r_*) > 0$, this follows from the proofs of Lemma 18 and Lemma 19. A proof that $f(r_*) > 0$ when $f(0) > \sqrt{2n}$ is given in Appendix B, where we study the linearized rotational self-shrinker differential equation near the sphere. In fact, we show that an outer quarter-sphere (viewed as a graph over the x-axis) has a local maximum and no local minima in the first quadrant. Therefore, we have the following result.

Proposition 12. *An outer quarter-sphere intersects the sphere exactly once before it crosses the r-axis.*

Appendix B: A Legendre type differential equation

In this appendix, we study the behavior of quarter-spheres near the sphere. Following the analysis in Appendix A of [21], where the $n = 2$ case is treated, we show that the linearization of the rotational self-shrinker differential equation near the sphere is a Legendre type differential equation. An analysis of this differential equation shows that outer quarter-spheres in the first quadrant intersect the r-axis with positive slope, and inner quarter-spheres in the first quadrant intersect the r-axis with negative slope.

Writing the rotational self-shrinker differential equation in polar coordinates $\rho = \rho(\phi)$, where $\rho = \sqrt{x^2+r^2}$ and $\phi = \arctan(r/x)$, we have

$$\rho'' = \frac{1}{\rho} \left\{ \rho'^2 + \left(\rho^2 + \rho'^2\right) \left[n - \frac{\rho^2}{2} - (n-1) \frac{\rho'}{\rho \tan\phi} \right] \right\}. \tag{17}$$

In these coordinates, the sphere corresponds to the constant solution $\rho = \sqrt{2n}$. We note that this equation has a singularity when $\phi = 0$ due to the $1/\tan\phi$ term.

Making the substitution $\psi = 1 - \cos\phi$, we can write equation (17) as

$$\begin{aligned} \psi \frac{d^2\rho}{d\psi^2} = {} & \frac{1}{\rho(2-\psi)} \left(\rho^2 + \psi(2-\psi) \left(\frac{d\rho}{d\psi} \right)^2 \right) \left[n - \frac{\rho^2}{2} - (n-1) \frac{(1-\psi)}{\rho} \frac{d\rho}{d\psi} \right] \\ & + \frac{\psi}{\rho} \left(\frac{d\rho}{d\psi} \right)^2 - (1-\psi) \frac{d\rho}{d\psi}, \end{aligned} \tag{18}$$

which has the form of the singular Cauchy problem studied in [4] (where ψ is the time variable). Applying Theorem 2.2 in [4] to (18), shows that the solution $\rho(\phi,\epsilon)$ to (17) with $\rho(0,\epsilon) = \sqrt{2n} + \epsilon$ and $\frac{d\rho}{d\phi}(0,\epsilon) = 0$ depends smoothly on (ϕ,ϵ) in a neighborhood of $(0,0)$. It then follows from the smooth dependence on initial conditions (away from the singularity at $\phi = 0$) for solutions to (17) that $\rho(\phi,\epsilon)$ is smooth when $\phi \in [0,\pi/2]$ and ϵ is close to 0.

In order to understand the behavior of $\rho(\phi,\epsilon)$ when ϵ is close to 0, we study the linearization of the rotational self-shrinker differential equation near the sphere $\rho(\phi,0) = \sqrt{2n}$. We define w by

$$w(\phi) = \frac{d}{d\epsilon}\Big|_{\epsilon=0} \rho(\phi,\epsilon).$$

Then w satisfies the (singular) linear differential equation:

$$w'' = -\frac{n-1}{\tan\phi} w' - 2nw, \tag{19}$$

with $w(0) = 1$ and $w'(0) = 0$. We will show that $w(\pi/2) < 0$ and $w'(\pi/2) < 0$.

Lemma 20. *Let w be the solution to* (19) *with $w(0) = 1$ and $w'(0) = 0$. Then $w(\pi/2) < 0$ and $w'(\pi/2) < 0$.*

Proof. We begin by making the substitution $\xi = \cos\phi$, which turns (19) into the following Legendre type differential equation:

$$(1-\xi^2)\frac{d^2w}{d\xi^2} = n\xi\frac{dw}{d\xi} - 2nw, \tag{20}$$

with the initial conditions at $\xi = 1$:

$$w(1) = 1, \qquad \frac{dw}{d\xi}(1) = 2.$$

To prove the lemma, we need to show that $w = w(\xi)$ satisfies $w(0) < 0$ and $\frac{dw}{d\xi}(0) > 0$.

Taking derivatives of (20) we have the following second order differential equations:

$$(1-\xi^2)\frac{d^3w}{d\xi^3} = (n+2)\xi\frac{d^2w}{d\xi^2} - n\frac{dw}{d\xi}, \tag{21}$$

$$(1-\xi^2)\frac{d^4w}{d\xi^4} = (n+4)\xi\frac{d^3w}{d\xi^3} + 2\frac{d^2w}{d\xi^2}. \tag{22}$$

It follows from (20) and (21) that

$$\frac{d^2w}{d\xi^2}(1) = \frac{2n}{n+2}, \qquad \frac{d^3w}{d\xi^3}(1) = -\frac{4n}{(n+2)(n+4)}.$$

We also note that the differential equation (22) for $\frac{d^2w}{d\xi^2}$ satisfies a maximum principle.

An analysis of the possible values of $\frac{d^2w}{d\xi^2}(0)$ and $\frac{d^3w}{d\xi^3}(0)$ shows that $\frac{d^2w}{d\xi^2}(0) > 0$ and $\frac{d^3w}{d\xi^3}(0) < 0$ are the only conditions that agree with the initial conditions at $\xi = 1$. For example, if $\frac{d^2w}{d\xi^2}(0) < 0$ and $\frac{d^3w}{d\xi^3}(0) > 0$, then the conditions $\frac{d^2w}{d\xi^2}(1) > 0$

and $\frac{d^3w}{d\xi^3}(1) < 0$ imply that $\frac{d^2w}{d\xi^2}$ achieves a positive maximum on $[0,1]$ at an interior point, which contradicts the maximum principle.

Since $\frac{d^2w}{d\xi^2}(0) > 0$ and $\frac{d^3w}{d\xi^3}(0) < 0$, it follows from (20) and (21) that $w(0) < 0$ and $\frac{dw}{d\psi}(0) > 0$. Regarding $w = w(\phi)$ as a function of ϕ, this says that $w(\pi/2) < 0$ and $w'(\pi/2) < 0$, which proves the lemma. □

Now we can prove the assertion about quarter-spheres made at the beginning of this appendix.

Proposition 13. *An outer quarter-sphere in the first quadrant intersects the r-axis with positive slope, and an inner quarter-sphere in the first quadrant intersects the r-axis with negative slope.*

Proof. It follows from Lemma 20 that the proposition is true for the quarter-sphere $Q[x_0]$ when x_0 is close to $\sqrt{2n}$. In fact, when x_0 is close to $\sqrt{2n}$, we know that $Q[x_0]$ is C^2 close to the sphere in the first quadrant, and applying Lemma 20 we have the following description of the shape of $Q[x_0]$ in the first quadrant: If $Q[x_0]$ is an inner quarter-sphere, then it is strictly convex and monotone in the first quadrant, and if $Q[x_0]$ is an outer quarter-sphere, then it is strictly convex with a local maximum in the first quadrant.

To prove the proposition in general, we first consider the case of inner quarter-spheres. Suppose to the contrary that some inner quarter-sphere intersects the r-axis with non-negative slope, and let x_0 be the first $x_0 < \sqrt{2n}$ with this property. It follows from the previous description of the shape of quarter-spheres near the sphere that $Q[x_0]$ is convex in the first quadrant and intersects the r-axis perpendicularly. Such a quarter-sphere corresponds to a (closed) convex self-shrinker that is not the sphere, which contradicts Huisken's theorem for mean-convex self-shrinkers.

Next, we consider the case of outer quarter-spheres. As in the previous case, suppose to the contrary that some outer quarter-sphere intersects the r-axis with non-positive slope, and let x_0 be the first $x_0 > \sqrt{2n}$ with this property. It again follows from the previous description of the shape of quarter-spheres near the sphere that $Q[x_0]$ intersects the r-axis perpendicularly; however, $Q[x_0]$ may not be convex in the first quadrant. We claim that the self-shrinker corresponding to $Q[x_0]$ is mean-convex. Writing $Q[x_0]$ as the graph of $u(x)$, where u is a solution to (4), it is sufficient to show that $\Psi(x) = xu' - u$ does not vanish for $0 \le x < x_0$. Since $\Psi(0) < 0$ and $\Psi(x_0) = -\infty$, we need to show that $\Psi < 0$. If Ψ has a non-negative maximum at some point $x_1 \in (0, x_0)$, then

$$0 = \Psi'(x_1) = x_1 u''(x_1) = x_1 \left(1 + u'(x_1)^2\right) \left[\frac{\Psi(x_1)}{2} + \frac{n-1}{u(x_1)}\right] > 0,$$

which is a contradiction. Therefore, $\Psi < 0$ and the self-shrinker corresponding to $Q[x_0]$ is mean-convex, which contradicts Huisken's theorem for mean-convex self-shrinkers.

We conclude that the first graphical component of an outer quarter-sphere $Q[x_0]$ with $x_0 > \sqrt{2n}$ intersects the r-axis with positive slope, and the first graphical component of an inner quarter-sphere $Q[x_0]$ with $0 < x_0 < \sqrt{2n}$ intersects the r-axis with negative slope. □

Appendix C: Pictures of profile curves

Here are some pictures of profile curves for immersed self-shrinkers with rotational symmetry.

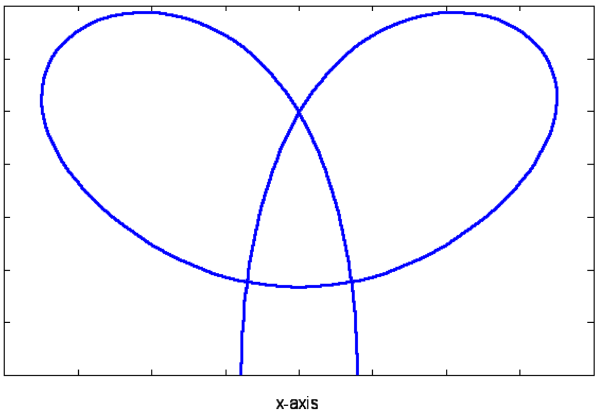

Figure 3. A profile curve whose rotation about the x-axis is an immersed sphere self-shrinker.

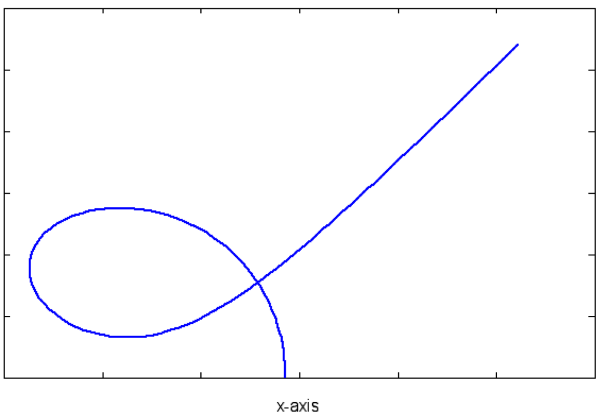

Figure 4. A profile curve with a trumpet end whose rotation about the x-axis is an immersed plane self-shrinker.

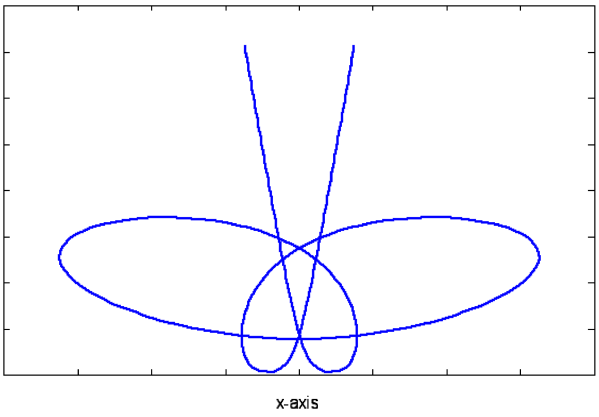

FIGURE 5. A profile curve with trumpet ends whose rotation about the x-axis is an immersed cylinder self-shrinker.

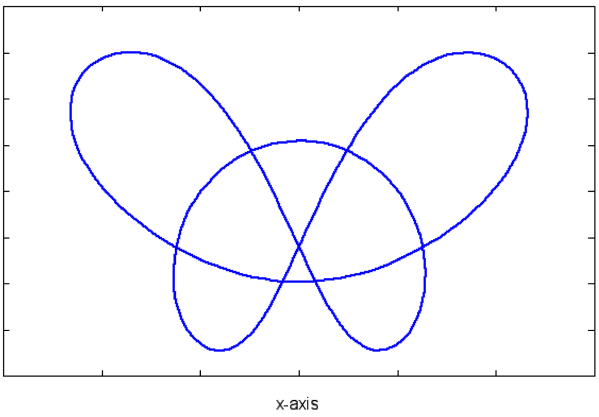

FIGURE 6. A profile curve whose rotation about the x-axis is an immersed torus self-shrinker.

REFERENCES

[1] U. Abresch and J. Langer, *The normalized curve shortening flow and homothetic solutions*, J. Differential Geom. **23** (1986), no. 2, 175–196. MR845704

[2] F. J. Almgren Jr., *Some interior regularity theorems for minimal surfaces and an extension of Bernstein's theorem*, Ann. of Math. (2) **84** (1966), 277–292. MR0200816

[3] Sigurd B. Angenent, *Shrinking doughnuts*, Nonlinear diffusion equations and their equilibrium states, 3 (Gregynog, 1989), Progr. Nonlinear Differential Equations Appl., vol. 7, Birkhäuser Boston, Boston, MA, 1992, pp. 21–38. MR1167827

[4] M. S. Baouendi and C. Goulaouic, *Singular nonlinear Cauchy problems*, J. Differential Equations **22** (1976), no. 2, 268–291. MR0435564

[5] Simon Brendle, *Embedded self-similar shrinkers of genus 0*, Ann. of Math. (2) **183** (2016), no. 2, 715–728, DOI 10.4007/annals.2016.183.2.6. MR3450486

[6] David L. Chopp, *Computation of self-similar solutions for mean curvature flow*, Experiment. Math. **3** (1994), no. 1, 1–15. MR1302814

[7] Tobias H. Colding and William P. Minicozzi II, *Generic mean curvature flow I: generic singularities*, Ann. of Math. (2) **175** (2012), no. 2, 755–833, DOI 10.4007/annals.2012.175.2.7. MR2993752

[8] Manfredo P. do Carmo, *Differential geometry of curves and surfaces*, Prentice-Hall, Inc., Englewood Cliffs, N.J., 1976. Translated from the Portuguese. MR0394451

[9] G. Drugan, *Embedded S^2 self-shrinkers with rotational symmetry*, preprint.

[10] Gregory Drugan, *An immersed S^2 self-shrinker*, Trans. Amer. Math. Soc. **367** (2015), no. 5, 3139–3159, DOI 10.1090/S0002-9947-2014-06051-0. MR3314804

[11] Klaus Ecker, *Regularity theory for mean curvature flow*, Progress in Nonlinear Differential Equations and their Applications, 57, Birkhäuser Boston, Inc., Boston, MA, 2004. MR2024995

[12] Klaus Ecker and Gerhard Huisken, *Mean curvature evolution of entire graphs*, Ann. of Math. (2) **130** (1989), no. 3, 453–471, DOI 10.2307/1971452. MR1025164

[13] C. L. Epstein and M. I. Weinstein, *A stable manifold theorem for the curve shortening equation*, Comm. Pure Appl. Math. **40** (1987), no. 1, 119–139, DOI 10.1002/cpa.3160400106. MR865360

[14] M. Gage and R. S. Hamilton, *The heat equation shrinking convex plane curves*, J. Differential Geom. **23** (1986), no. 1, 69–96. MR840401

[15] David Gilbarg and Neil S. Trudinger, *Elliptic partial differential equations of second order*, Classics in Mathematics, Springer-Verlag, Berlin, 2001. Reprint of the 1998 edition. MR1814364

[16] Matthew A. Grayson, *The heat equation shrinks embedded plane curves to round points*, J. Differential Geom. **26** (1987), no. 2, 285–314. MR906392

[17] Hoeskuldur P. Halldorsson, *Self-similar solutions to the curve shortening flow*, Trans. Amer. Math. Soc. **364** (2012), no. 10, 5285–5309, DOI 10.1090/S0002-9947-2012-05632-7. MR2931330

[18] Philip Hartman, *Ordinary differential equations*, John Wiley & Sons, Inc., New York-London-Sydney, 1964. MR0171038

[19] Heinz Hopf, *Differential geometry in the large*, 2nd ed., Lecture Notes in Mathematics, vol. 1000, Springer-Verlag, Berlin, 1989. Notes taken by Peter Lax and John W. Gray; With a preface by S. S. Chern; With a preface by K. Voss. MR1013786

[20] Gerhard Huisken, *Asymptotic behavior for singularities of the mean curvature flow*, J. Differential Geom. **31** (1990), no. 1, 285–299. MR1030675

[21] N. Kapouleas, S. J. Kleene, and N. M. Møller, *Mean curvature self-shrinkers of high genus: Non-compact examples*, preprint. Available at arXiv:1106.5454.

[22] Stephen Kleene and Niels Martin Møller, *Self-shrinkers with a rotational symmetry*, Trans. Amer. Math. Soc. **366** (2014), no. 8, 3943–3963, DOI 10.1090/S0002-9947-2014-05721-8. MR3206448

[23] N. M. Møller, *Closed self-shrinking surfaces in R^3 via the torus*, preprint. Available at arXiv:1111.7318.

[24] Xuan Hien Nguyen, *Construction of complete embedded self-similar surfaces under mean curvature flow. I*, Trans. Amer. Math. Soc. **361** (2009), no. 4, 1683–1701, DOI 10.1090/S0002-9947-08-04748-X. MR2465812

[25] Xuan Hien Nguyen, *Construction of complete embedded self-similar surfaces under mean curvature flow. II*, Adv. Differential Equations **15** (2010), no. 5-6, 503–530. MR2643233

[26] Xuan Hien Nguyen, *Construction of complete embedded self-similar surfaces under mean curvature flow, Part III*, Duke Math. J. **163** (2014), no. 11, 2023–2056, DOI 10.1215/00127094-2795108. MR3263027

[27] Lu Wang, *A Bernstein type theorem for self-similar shrinkers*, Geom. Dedicata **151** (2011), 297–303, DOI 10.1007/s10711-010-9535-2. MR2780753

Department of Mathematics, University of Washington, Seattle, Washington 98195
E-mail address: drugan@math.washington.edu

Department of Mathematics, Massachusetts Institute of Technology, Cambridge, Massachusetts 02139
E-mail address: skleene@math.mit.edu